PHYSICAL REVIEW A VOLUME 23, NUMBER 3 MARCH 1981

Many-body theory of core-valence excitations

A. Barth and L. S. Cederbaum
Lehrstuhl für Theoretische Chemie, Institut für Physikalische Chemie, Universität Heidelberg, 6900 Heidelberg, Germany

(Received 8 July 1980)

A many-body theory is presented based on an electronic Hamiltonian appropriate for describing core-valence excitation processes. It is shown that the core polarization propagator satisfies a factorization theorem relating this propagator to the product of two one-particle Green's functions, namely, a core Green's function and a valence Green's function which is calculated in the field of a time-dependent core potential. A diagrammatic theory for this valence Green's function is developed. The core-valence excitation energy is decomposed into relaxation and correlation contributions up to second order. A physical interpretation of this decomposition is given and the relationship between the analytical expressions and the various diagrams is pointed out. A general order analysis of relaxation and correlation terms is performed making use of the factorization theorem. An illustrative model is presented which allows an exact diagrammatic calculation of the valence Green's function with the time-dependent core potential via the Dyson equation. The analogy between the spectral function of our model and the spectral function of x-ray emission spectra of solids is discussed.

I. INTRODUCTION

The study of electron excitation processes has been a famous subject over the last few years both for experimentalists and theoreticians. Although the main spectroscopic interest is focused upon the valence region, the investigation of core processes has gained an increasing importance, especially in connection with the development of synchrotron light sources[1] and the extension of electron-energy-loss spectroscopy[2] to the high-energy region. The progress in the development of experimental techniques has raised a great number of problems concerning the interpretation of spectra and thus stimulated the theoretical interest in the subject. In the case of solids one usually introduces a model Hamiltonian[3,4] which accounts for the effects to be explained. For atoms and molecules there exist computational methods which permit a rather accurate description of the experimental spectra. Besides semiempirical procedures, the so-called *ab initio* methods[5] have gained an increasing importance. The excitation energies can, in principle, be obtained by performing separate Hartree-Fock (HF) computations for the initial and final state (ΔSCF). This accounts solely for the relaxation (reorganization) effect of the orbitals caused by the rearrangement of the electronic charge distribution upon the transition. Although this is the main contribution in the case of core excitations, the corrections due to correlation effects have to be considered, too. Moreover, there are certain excited states which cannot be evaluated in the simple HF scheme. To overcome these shortcomings one usually improves the numerical data by performing a configuration interaction (CI) calculation. Hitherto, however, only a few CI calculations on core-valence excitations have been performed.[6] Owing to various drawbacks, as slow convergence, different treatment of initial and final states, and the size-consistency problem,[7] the CI method is not quite satisfactory. The Green's function formalism,[8-17] on the other hand, gives complementary physical insight into the excitation process by calculating transition energies and line intensities directly.

In the mathematical framework of the many-body theory a description of excitations requires the knowledge of the particle-hole or polarization propagator. This is a special component of the two-particle Green's function satisfying a rather complicated multiple integral equation called the Bethe-Salpeter equation.[8-11,15,18] In the present contribution it is shown that in the particular case of excitations originating from deep core holes the polarization propagator satisfies an important factorization theorem. In time-space the core polarization propagator is equal to the product of two one-particle Green's functions, namely, a core Green's function and a valence Green's function with a time-dependent potential. The core-valence excitation spectrum is then obtained by convoluting these functions. We have thus reduced the problem of evaluating a two-particle Green's function to the problem of calculating two one-particle Green's functions. The factorization theorem allows us to treat the core-valence excitation as two independent processes, but at the cost of introducing a time-dependent potential into the Hamiltonian of the valence Green's function.

The general notations and equations required for the analysis of core-valence excitations are presented in Sec. II A. In Sec. II B the excitation energy up to second order is decomposed into relaxation and correlation contributions. The connection of this analysis to a diagrammatic approach is discussed. The Hamiltonian appropriate for the description of core processes is introduced in Sec. III A. For this Hamiltonian the Bethe-Salpeter equation for core-valence excitations is analyzed in Sec. III B. In Sec. III C the factorization theorem is introduced and discussed in detail and the valence Green's function with the time-dependent potential is interpreted. This section contains the main results of our analysis. In Sec. III D we discuss the diagrammatic theory for the valence Green's function and derive the appropriate Dyson equation. In Sec. III E we return to the discussion of Sec. II B and analyze the decomposition of the core-valence excitation into relaxation and correlation contributions up to second order for the case of our Hamiltonian. The analytic expressions are related to simple diagrams. An interpretation of the various contributions is given. An illustrative model is analyzed in detail in Sec. IV. This model demonstrates in compact form the main features of our analysis. The close relationship of our theory to the theory of core-valence excitations in solids is also discussed in Sec. IV.

II. THE EXCITATION SPECTRUM

A. The particle-hole propagator

The excitation process is in general well described by using Fermi's Golden Rule. Then the excitation spectrum $P(\omega)$ as a function of ω is given by[14]

$$P(\omega) \sim -\sum_{ijkl} \tau^*_{kl}\tau_{ji}\,\mathrm{Im}[i\Pi_{ijkl}(-\hbar\omega_0 - i\eta)]\,\delta(\omega - E_e)\,, \tag{1}$$

where $\tau_{ij} = \langle\phi_i|v|\phi_j\rangle$ are the matrix elements of the external perturbation potential which induces the transition process. The matrix elements are taken between the orbitals of our chosen basis set $\{\phi_i\}$. If the excitation is induced by photons the perturbation potential reads

$$V = \sum_n \underline{A}_n \cdot \underline{P}_n$$

which is the scalar product of the external field at the nth electron and the momentum of this electron. $\hbar\omega_0$ is the photon energy or the kinetic energy of the impact particle and E_e is the excitation energy. $\Pi_{ijkl}(\omega)$ is the Fourier transform of the particle-hole component of the two-particle Green's function[8-13,15-18] and η is a positive infinitesimal. The particle-hole Green's function contains all the many-body effects and a calculation of this function enables us to evaluate the excitation spectrum. Thus the natural task will be to derive an equation which determines the particle-hole Green's function.

Restricting ourselves to the pure electronic problem of a many-electron molecule the corresponding Hamiltonian in second quantized notation is given by

$$H = \sum_i \epsilon_i a_i^\dagger a_i + \sum_{ij} v_{ij} a_i^\dagger a_j + \tfrac{1}{2}\sum_{ijkl} V_{ijkl} a_i^\dagger a_j^\dagger a_l a_k\,. \tag{2}$$

Here ϵ_i, v_{ij}, and V_{ijkl} are the matrix elements of an unperturbed Hamiltonian H_0, a one-particle potential v, and of the Coulomb interaction between the electrons

$$V_{ijkl} = \int dr_1 dr_2 \phi_i^*(r_1)\phi_j^*(r_2)\,|r_1 - r_2|^{-1}\phi_k(r_1)\phi_l(r_2)\,.$$

The potential v can, in principle, include an external potential. $\{\phi_i\}$ is any orthogonal basis of spin orbitals that diagonalizes H_0. $a_i(a_i^\dagger)$ is a destruction (creation) operator for a one-particle state.

Without loss of generality H_0 is assumed to be the Hartree-Fock operator. In this case the ϵ_i become the HF orbital energies and, if no external potential is included, v_{ij} is given by

$$v_{ij} = -\sum_k V_{ik[jk]} n_k\,,$$
$$V_{ij[kl]} = V_{ijkl} - V_{ijlk}\,.$$

n_k is the occupation number of the orbital ϕ_k in the HF ground state, i.e., $n_k = 1$ if ϕ_k is occupied in the HF ground state and $n_k = 0$ otherwise. It is also useful to define the quantity $\bar{n}_k = 1 - n_k$.

If H_0 is chosen to be the spin unrestricted[19] HF operator the formalism is the same in the closed- and open-shell case. On the other hand, if H_0 is the spin restricted[20] HF operator the choice of v_{ij} in the open-shell case is ambiguous. The following discussion is restricted to the closed-shell case.

For a theoretical analysis of electronic excitations we consider the particle-hole Green's function,[10] also known as polarization or particle-hole propagator. If the Hamiltonian is not explicitly time-dependent this function depends only on the time difference which we denote by t. The particle-hole propagator reads (normalizing $\langle\Psi_0|\Psi_0\rangle$ to 1)

$$i\Pi_{ijkl}(t) = \langle\Psi_0|\,T[a_j^\dagger(t)a_i(t)a_k^\dagger a_l]\,|\Psi_0\rangle\,, \tag{3}$$

where we have adapted the notation of Ref. 10. T is called Wick's time ordering operator and $a_i(t) = e^{iHt}a_i e^{-iHt}$ denotes the destruction operator in the Heisenberg picture. $|\Psi_0\rangle$ is the exact ground state of N particles. $\Pi(t)$ describes a particle-hole propagation between the times 0 and t.

To obtain a deeper insight into the physical meaning of this function it is necessary to exhibit explicitly its energy dependence. After inserting a complete set of N particle eigenstates $\{|\Psi_n^N\rangle\}$ and subsequent transformation to ω space, the Lehmann representation is obtained,[21]

$$\Pi_{ijkl}(\omega)=\sum_n \frac{\langle\Psi_0|a_j^\dagger a_i|\Psi_n^N\rangle\langle\Psi_n^N|a_k^\dagger a_l|\Psi_0\rangle}{\omega-(E_n^N-E_0)+i\eta} - \sum_n \frac{\langle\Psi_0|a_k^\dagger a_l|\Psi_n^N\rangle\langle\Psi_n^N|a_j^\dagger a_i|\Psi_0\rangle}{\omega+(E_n^N-E_0)-i\eta}, \tag{4}$$

where E_0 and E_n^N are the energies of the ground and excited states and η is a positive infinitesimal. $\Pi_{ijkl}(\omega)$ is a mermorphic function whose poles are the excitation energies and whose residues are the transition probabilities. Both terms contain equivalent information but the poles lie on different sides of the complex plane. The case of noninteracting fermions is easily obtained,

$$\Pi^0_{ijkl}(\omega)=\delta_{ik}\delta_{jl} \times\left(\frac{\bar{n}_i n_j}{\omega-(\epsilon_i-\epsilon_j)+i\eta}-\frac{n_i\bar{n}_j}{\omega+(\epsilon_j-\epsilon_i)-i\eta}\right). \tag{5}$$

In this simple case the excitation energies are just the differences between the ϵ's and the transition probabilities are 0 or 1, respectively.

We can define a new quantity

$$i\Pi_{ijkl}(t,-t')\equiv\langle\Psi_0|T[a_j^\dagger(t')a_i(t)a_k^\dagger a_l]|\Psi_0\rangle, \tag{6}$$

which in analogy to the Dyson equation of the one-particle Green's function, satisfies an equation in time-space called the Bethe-Salpeter equation[8-12,15,18]

$$(-i)\Pi_{ijkl}(t,-t')=iG_{ik}(t)iG_{lj}(-t') + \sum_{\alpha\beta\gamma\delta}\int dt_1\cdots\int dt_4\, iG_{i\alpha}(t-t_1)iG_{\beta j}(t_2-t')iK_{\alpha\beta\gamma\delta}(t_1,t_2,t_3,t_4)(-i)\Pi_{\gamma\delta kl}(t_3,-t_4). \tag{7}$$

This auxiliary function depends on two different times t and t' and it is related to the polarization propagator $\Pi(t)$ by

$$\Pi(t)=\lim_{t'\to t}\Pi(t,-t').$$

K is called the particle-hole scattering kernel[10] or amplitude[12] corresponding to the self-energy Σ in the one-particle case. The K matrix depends on four different times which can be combined to three time differences, e.g.,

$$K(t_1,t_2,t_3,t_4)\equiv K(t_1-t_3,t_4-t_2,t_1-t_2).$$

Because of the complicated structure of the Bethe-Salpeter equation, it is clear that its Fourier transformation cannot lead to an algebraic equation in ω space, but rather to an integral equation. Introducing the Fourier transformations as

$$G_{ij}(\omega)=\int dt\, e^{i\omega t}G_{ij}(t), \tag{8a}$$

$$\Pi^0_{ijkl}(\omega',\omega'')\equiv -i\int dt\, d(-t')e^{i\omega' t}e^{i\omega''(-t')}G_{ik}(t)G_{lj}(-t') = -iG_{ik}(\omega')G_{lj}(\omega''), \tag{8b}$$

$$\Pi_{ijkl}(\omega',\omega'')=\int dt\, d(-t')e^{i\omega' t}e^{i\omega''(-t')}\Pi_{ijkl}(t,-t'), \tag{8c}$$

$$K_{ijkl}(\omega',\omega'',\omega''')=\int d(t_1-t_3)d(t_4-t_2)d(t_1-t_2)e^{i\omega'(t_1-t_3)}e^{i\omega''(t_4-t_2)} \times e^{i\omega'''(t_1-t_2)}K_{ijkl}(t_1-t_3,t_4-t_2,t_1-t_2), \tag{8d}$$

we finally arrive at the following integral equation:

$$\Pi(\omega',\omega'-\omega)=\Pi^0(\omega',\omega'-\omega)\left(1+\int\frac{d\omega_1}{2\pi}K(\omega_1,\omega_1-\omega,\omega'-\omega_1)\Pi(\omega_1,\omega_1-\omega)\right). \tag{9}$$

The final result follows from

$$\Pi(\omega) = \int \frac{d\omega'}{2\pi}\, \Pi(\omega', \omega' - \omega)\,. \tag{10}$$

Equation (9) is an integral equation in several dimensions and is, therefore, very difficult to solve for any realistic physical system. In order to proceed, the following simplifying approximation of the particle-hole scattering kernel is commonly made:

$$K(\omega_1, \omega_1 - \omega, \omega' - \omega_1) \approx K(\omega)\,. \tag{11a}$$

In time-space, this approximation corresponds to[18]

$$K(t_1 - t_3, t_4 - t_2, t_1 - t_2) \approx K(t_1 - t_3)\delta(t_1 - t_2)\delta(t_3 - t_4)\,. \tag{11b}$$

Now the integration (10) can be performed and a Dyson-type equation is obtained[10]

$$\Pi(\omega) = \Pi^0(\omega) + \Pi^0(\omega)K(\omega)\Pi(\omega)\,. \tag{12}$$

This equation can be transformed to a non-Hermitean eigenvalue problem. The zero eigenvalues of $\Pi^{-1}(\omega)$ are the requested excitation energies and the eigenvector coefficients yield the transition probabilities

$$\sum_{\alpha\beta} [\Pi^0(\omega)^{-1} - K(\omega)]_{ij\alpha\beta} C_{\alpha\beta} = 0\,. \tag{13}$$

The simplest approximations for solving this set of linear equations are the Tamm-Dancoff (TDA) and random-phase approximation (RPA).[10] The coupled equations of the RPA are obtained by substituting $K_{ijkl}(\omega)$ by its first-order approximation $-V_{il[kj]}$ and replacing $\Pi^0_{ijkl}(\omega)$ defined by Eqs. (8b) and (10) by its noninteracting form given in Eq. (5) as

$$(\omega - \epsilon_i + \epsilon_j)\bar{n}_i n_j C_{ij} + \sum_{\alpha,\beta} V_{i\beta[\alpha j]}\bar{n}_i n_j (\bar{n}_\alpha n_\beta + n_\alpha \bar{n}_\beta) C_{\alpha\beta} = 0\,, \tag{14a}$$

$$(\omega + \epsilon_j - \epsilon_i) n_i \bar{n}_j C_{ij} - \sum_{\alpha,\beta} V_{i\beta[\alpha j]} n_i \bar{n}_j (\bar{n}_\alpha n_\beta + n_\alpha \bar{n}_\beta) C_{\alpha\beta} = 0\,. \tag{14b}$$

If we restrict the indices i, α to particles and j, β to holes, referring to unoccupied and occupied states in the HF ground state, Eqs. (14) decouple and we are led to the TDA equations

$$(\omega - \epsilon_i + \epsilon_j)\bar{n}_i n_j C_{ij} + \sum_{\alpha,\beta} V_{i\beta[\alpha j]}\bar{n}_i n_j \bar{n}_\alpha n_\beta C_{\alpha\beta} = 0\,. \tag{15}$$

In the TDA only one particle-hole pair is present at any instant of time whereas in the RPA no such restriction is imposed. Consequently only the latter contains a part of the ground-state correlation energy.

A diagrammatic perturbation theory can be derived for the polarization propagator via Wick's theorem. This is done by transforming (3) into the interaction picture[10]

$$\begin{aligned} i\Pi_{ijkl}(t) &= \sum_{n=0}^{\infty} \frac{(-i)^n}{n!} \int dt_1 \cdots \int dt_n \langle \Phi_0 | T[H'(t_1)\cdots H'(t_n) a_j^\dagger(t) a_i(t) a_k^\dagger a_l] | \Phi_0 \rangle\,, \\ H'(t_1) &= \tfrac{1}{2} \sum_{ijkl} V_{ijkl} N[a_i^\dagger(t_1) a_j^\dagger(t_1) a_l(t_1) a_k(t_1)]\,. \end{aligned} \tag{16}$$

$|\Phi_0\rangle$ is the HF ground state, $H'(t_1)$ is the perturbation operator in the interaction picture, and $N[\cdots]$ means normal product implicating that H_0 is the HF operator. Our choice of the unperturbed Hamiltonian H_0 provides a convenient starting point for many-body calculations because H_0 is explicitly diagonal and $\langle \Phi_0 | H' | \Phi_0 \rangle$ vanishes. Making use of Wick's Theorem one obtains a perturbation expansion for $\Pi(t)$ which can be expressed in diagrams. This has been discussed by several authors[10,15,16] and we just present those results here which we need for our analysis.

The graphical symbols we use are shown in Fig. 1. It is also useful to define the unperturbed one-particle Green's function $G^0_{kk'}(t_1 - t_2)$

$$G^0_{kk'}(t_1 - t_2) = (-i)\delta_{kk'}[\bar{n}_k \Theta(t_1 - t_2) - n_k \Theta(t_2 - t_1)]\, e^{-i\epsilon_k(t_1 - t_2)}\,.$$

To obtain an idea of how equations can be represented by diagrams, the Bethe-Salpeter equation is shown in Fig. 2. The diagrams of $\Pi(t)$ can be classified as connected and disconnected diagrams. All diagrams of the polarization propagator are obtained by iterating $\Pi(t, -t')$ in the Bethe-Salpeter equation and performing the limit $t' \to t$ afterwards.

We introduce a new matrix $\hat{K}$ containing all topologically distinct connected diagrams with four external indices (two incoming and two outgoing indices) which cannot be separated into two pieces by cutting a single particle (hole) line (reducible diagrams). Then the K matrix contains all diagrams of $\hat{K}$ which cannot be separated into two pieces by cutting a particle and a hole line at the same time level (irreducible diagrams). Subsequently we give the rules to evaluate the nth order

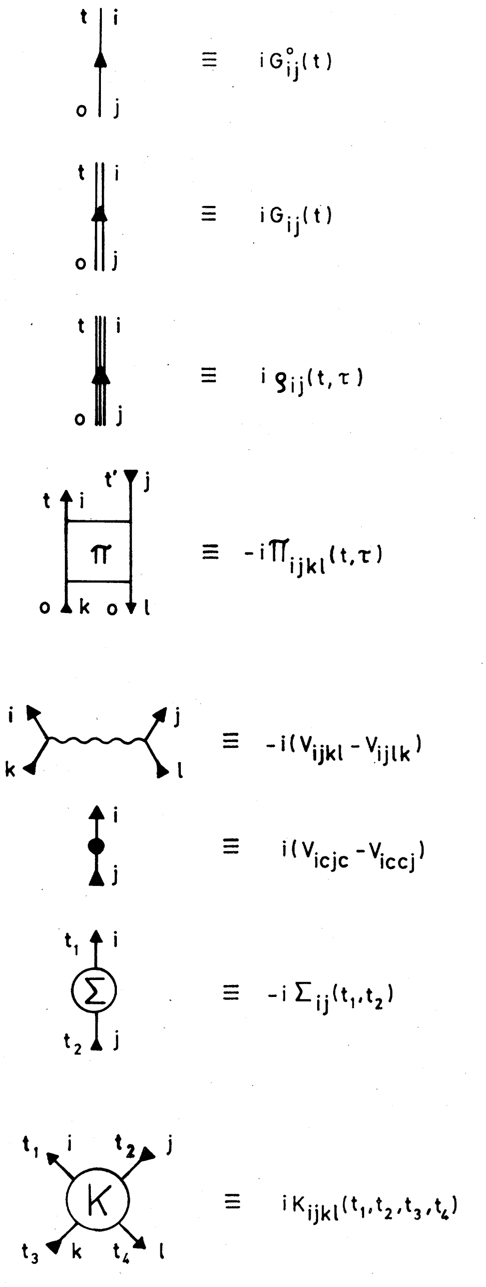

FIG. 1. Definition of the graphical symbols.

contribution to the particle-hole scattering kernel K in time-space.

(1) Draw all topologically distinct connected irreducible diagrams with $n(\geq 1)$ interaction lines $V_{ij[kl]}$ and $2n-2$ unperturbed Green's functions $G^0_{kk'}$ containing four external indices (two "in" and two "out").

(2) Multiply the Green's functions and the interaction lines of a given diagram.

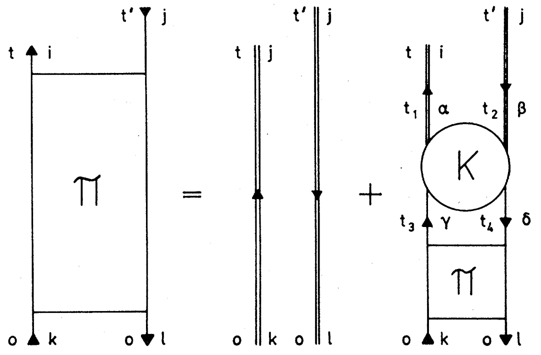

FIG. 2. Graphical representation of the Bethe-Salpeter equation (7).

(3) Multiply with a factor $2^{-q}(-1)^F(-i)^{3n-1}$ where F is the number of closed fermion loops in the diagram, and q is the number of permutations of two G^0 lines in the diagram leaving the diagram unchanged.

(4) Integrate over all internal time variables and sum over all internal indices.

The rules enable us to evaluate the particle-hole scattering kernel in time-space. The Fourier transformation of K is then obtained by using Eq. (8d). In order to arrive at the simplified form of the Bethe-Salpeter equation (12) one has to use Eq. (11b) where the δ functions reduce the number of independent time variables. The Fourier transformation (8d) is then easily performed and the result can directly be inserted into Eq. (12).

B. Analysis of the excitation energy in terms of relaxation and correlation contributions

In a Green's function approach the excitation energies are determined directly. An alternative approach is to evaluate the transition energies by separately calculating the energies of the ground state and the excited state. If both states are calculated by an HF procedure the result is called ΔSCF method. This approximation takes only the reorganization (relaxation) of the orbitals into account. For an accurate calculation the incorporation of the correlation effects is also important and has to be considered, too. This is usually done by the configuration interaction (CI) method. Thus, there are two corrections to Koopman's theorem caused by the reorganization and the change of correlation. A decomposition of the excitation energy into these different terms is, therefore, of interest. Our analysis of the excitation energy is closely related to that of the ionization energy which has been given by various authors.[22,23]

The HF ground-state energy and the HF energy of the excited state which results upon excitation from orbital x to orbital v, read

$$E_0^{\mathrm{HF}}=\sum_{i\neq x}\epsilon_i n_i+\epsilon_x$$

$$-\tfrac{1}{2}\sum_{ij\neq x}V_{ij[ij]}n_i n_j-\sum_i V_{ix[ix]}n_i\,, \tag{17a}$$

$$E_{x\to \mathrm{v}}^{\mathrm{HF}}=\sum_{i\neq x}\tilde{\epsilon}_i n_i+\tilde{\epsilon}_{\mathrm{v}}$$

$$-\tfrac{1}{2}\sum_{ij\neq x}\tilde{V}_{ij[ij]}n_i n_j-\sum_{i\neq x}\tilde{V}_{i\mathrm{v}[i\mathrm{v}]}n_i\,. \tag{17b}$$

$\tilde{\epsilon}_i$ and $V_{ij[ij]}$ are the matrix elements of the HF operator and of the Coulomb interaction between the electrons calculated in the relaxed field. A Rayleigh-Schrödinger perturbation expansion can be made for $\tilde{\epsilon}_i$ and $\tilde{\phi}_i$,

$$\tilde{\epsilon}_i=\epsilon_i+\epsilon_i^{(1)}+\epsilon_i^{(2)}+\cdots\,,$$

$$\tilde{\phi}_i=\phi_i+\phi_i^{(1)}+\phi_i^{(2)}+\cdots\,.$$

The HF operators for the excited state can be expressed via that for the ground state which serves now as the unperturbed Hamiltonian. The ΔSCF excitation energy can now easily be calculated up to second order,

$$\Delta E_{x\to \mathrm{v}}^{\mathrm{SCF}}=\epsilon_{\mathrm{v}}-\epsilon_x-V_{x\mathrm{v}[x\mathrm{v}]}+\sum_{i,j\neq x}\frac{|V_{i\mathrm{v}[j\mathrm{v}]}|^2}{\epsilon_j-\epsilon_i}\bar{n}_i n_j+\sum_{i\neq \mathrm{v},j}\frac{|V_{xi[xj]}|^2}{\epsilon_j-\epsilon_i}\bar{n}_i n_j+\sum_{i\neq \mathrm{v}}\frac{|V_{x\mathrm{v}[xi]}|^2}{\epsilon_{\mathrm{v}}-\epsilon_i}\bar{n}_i$$

$$+\sum_{i\neq x}\frac{|V_{i\mathrm{v}[x\mathrm{v}]}|^2}{\epsilon_i-\epsilon_x}n_i-2\sum_{ij}\frac{V_{ix[jx]}V_{j\mathrm{v}[i\mathrm{v}]}}{\epsilon_j-\epsilon_i}\bar{n}_i n_j\,. \tag{18}$$

To find the correlation energy up to second order ordinary Rayleigh-Schrödinger perturbation theory is used. For the ground state the correlation part reads

$$E_0^C=\tfrac{1}{4}\sum_{ijkl}\frac{|V_{ij[kl]}|^2}{\epsilon_i+\epsilon_j-\epsilon_k-\epsilon_l}n_i n_j\bar{n}_k\bar{n}_l\,. \tag{19a}$$

For the correlation energy of the excited state we obtain

$$E_{x\to \mathrm{v}}^C=\tfrac{1}{4}\sum_{ijkl}{}'\frac{|V_{ij[kl]}|^2}{\epsilon_i+\epsilon_j-\epsilon_k-\epsilon_l}n_i n_j\bar{n}_k\bar{n}_l+\tfrac{1}{2}\sum_{jkl}{}'\frac{|V_{\mathrm{v}j[kl]}|^2}{\epsilon_{\mathrm{v}}+\epsilon_j-\epsilon_k-\epsilon_l}n_j\bar{n}_k\bar{n}_l$$

$$+\tfrac{1}{2}\sum_{ijk}{}'\frac{|V_{ij[kx]}|^2}{\epsilon_i+\epsilon_j-\epsilon_k-\epsilon_x}n_i n_j\bar{n}_k+\sum_{ik}{}'\frac{|V_{i\mathrm{v}[xk]}|^2}{\epsilon_i+\epsilon_{\mathrm{v}}-\epsilon_x-\epsilon_k}n_i\bar{n}_k\,. \tag{19b}$$

The prime indicates that the hole indices do not include x and the particle indices do not include v. The change of the correlation energy due to the excitation is now given by

$$\Delta E_{x\to \mathrm{v}}^C=\tfrac{1}{2}\sum_{jkl}{}'\frac{|V_{\mathrm{v}j[kl]}|^2}{\epsilon_{\mathrm{v}}+\epsilon_j-\epsilon_k-\epsilon_l}(n_j\bar{n}_k\bar{n}_l+\bar{n}_j n_k n_l)+\tfrac{1}{2}\sum_{ijk}{}'\frac{|V_{ij[kx]}|}{\epsilon_i+\epsilon_j-\epsilon_k-\epsilon_x}(n_i n_j\bar{n}_k+\bar{n}_i\bar{n}_j n_k)$$

$$+\sum_{i,k}{}'\frac{|V_{i\mathrm{v}[xk]}|^2}{\epsilon_i+\epsilon_{\mathrm{v}}-\epsilon_x-\epsilon_k}(n_i\bar{n}_k+\bar{n}_i n_k)\,. \tag{20}$$

The total excitation energy is obtained by adding the changes caused by correlation and relaxation effects

$$\Delta E_{x\to \mathrm{v}}=\Delta E_{x\to \mathrm{v}}^{\mathrm{SCF}}+\Delta E_{x\to \mathrm{v}}^C\,.$$

In order to understand the meaning of the individual relaxation and correlation terms up to second order, a diagrammatic analysis via the Bethe-Salpeter equation (9) is made. A look at Fig. 2 which is a graphical illustration of Eq. (9) shows that Π consists of an unlinked term Π^0 and a linked term which is the multiple integral in this equation. The unlinked term is just a product of two one-particle Green's functions, which can be expanded individually up to second order and thus we obtain a contribution of zeroth and two different contributions of second order. Next we consider the linked term. Since the K matrix is at least of first order, Π^0 must be of zeroth order and Π can be of order zero or one which yields a first and a second-order term, respectively. If K is of second order both Π^0 and Π are of zeroth order and we obtain two other second-order terms. The summation of all these terms yields the polarization propagator up to second order in the electron interaction.

Now we can use Eq. (10), invert the polarization porpagator, and finally obtain

$$\Delta E_{x\to \mathrm{v}}=\epsilon_{\mathrm{v}}-\epsilon_x+\Sigma_{\mathrm{vv}}^{(2)}(\epsilon_{\mathrm{v}})-\Sigma_{xx}^{(2)}(\epsilon_x)+\hat{K}_{x\mathrm{v}x\mathrm{v}}(\epsilon_{\mathrm{v}},\epsilon_x,\epsilon_{\mathrm{v}}-\epsilon_x)\,, \tag{21}$$

where $\Sigma_{ii}^{(2)}(\epsilon_i)$ is the diagonal part of the 2nd order self-energy of the one-particle Green's function and K is defined in Sec. II A. There are six diagrams corresponding to Eq. (21) and they are shown in Fig. 3. From these diagrams one obtains the following expression

$$\begin{aligned}\Delta E_{x\to v} = {} & \epsilon_v - \epsilon_x - V_{xv[xv]} + \tfrac{1}{2}\sum_{ijk}\frac{|V_{vk[ij]}|^2}{\epsilon_v+\epsilon_k-\epsilon_i-\epsilon_j}(\bar{n}_i\bar{n}_j n_k + n_i n_j \bar{n}_k) \\ & + \tfrac{1}{2}\sum_{ijk}\frac{|V_{xk[ij]}|^2}{\epsilon_i+\epsilon_j-\epsilon_k-\epsilon_x}(n_i n_j \bar{n}_k + \bar{n}_i\bar{n}_j n_k) + \sum_{ij}\frac{|V_{vj[ix]}|^2}{\epsilon_v+\epsilon_j-\epsilon_i-\epsilon_x}(\bar{n}_i n_j - n_i\bar{n}_j) \\ & - 2\sum_{ij}\frac{V_{vi[vj]}V_{xj[xi]}}{\epsilon_j-\epsilon_i}\bar{n}_i n_j - \tfrac{1}{2}\sum_{ij}\frac{|V_{xv[ij]}|^2}{\epsilon_v+\epsilon_x-\epsilon_i-\epsilon_j}(\bar{n}_i\bar{n}_j - n_i n_j)\,. \end{aligned} \tag{22}$$

The sequence of the last six terms in this equation corresponds to the sequence of diagrams shown in Fig. 3. In order to proceed we decompose Figs. 3(b), 3(c), and 3(d) into time-ordered diagrams with distinct restrictions on the summation indices. For Fig. 3(b) this decomposition is demonstrated in Fig. 4. The corresponding analytical expression reads

$$\begin{aligned}\Sigma_{vv}^{(2)}(\epsilon_v) = {} & \tfrac{1}{2}\sum_{ij}\frac{|V_{vx[ij]}|^2}{\epsilon_v+\epsilon_x-\epsilon_i-\epsilon_j}\bar{n}_i\bar{n}_j + \sum_{j,k\neq x}\frac{|V_{vk[vj]}|^2}{\epsilon_k-\epsilon_j}\bar{n}_j n_k + \tfrac{1}{2}\sum_{\substack{ij\neq v\\ k\neq x}}\frac{|V_{vk[ij]}|^2}{\epsilon_v+\epsilon_k-\epsilon_i-\epsilon_j}\bar{n}_i\bar{n}_j n_k \\ & + \sum_{i,k}\frac{|V_{vk[ix]}|^2}{\epsilon_v+\epsilon_k-\epsilon_i-\epsilon_x}n_i\bar{n}_k + \tfrac{1}{2}\sum_{\substack{ij\neq x\\ k\neq v}}\frac{|V_{vk[ij]}|^2}{\epsilon_v+\epsilon_k-\epsilon_i-\epsilon_j}n_i n_j \bar{n}_k\,. \end{aligned} \tag{23}$$

As can be seen by a short inspection, several contributions of Eq. (22) cancel, e.g., the first subterm of the last term in Eq. (22) is compensated by the first term in Eq. (23). A closer inspection brings us back to Eqs. (18) and (20), but now we are able to relate the various sums in these equations to distinct time-ordered diagrams. The detailed diagrammatic discussion and the physical interpretation of these diagrams is postponed to Sec. III E, where we consider the case of core-valence excitations. Finally it should be noted that Eq. (12) cannot be used here because the terms in Figs. 3(e) and 3(f) yield a wrong contribution in this approximation.

III. THE CORE-VALENCE EXCITATION SPECTRUM

A. The Hamiltonian

In a theoretical treatment of the core problem it is useful to take into account explicitly the specific features of deep core holes. Because of the energetic differences and strong spatial separation of the core and valence orbitals it is, in general, assumed that the Hamiltonian is core-valence separable.[24] This means that the core and valence number operators N_c and N_v both commute with this Hamiltonian. The core-valence separable Hamiltonian H_{cv} is obtained from the full electronic Hamiltonian of Eq. (2) by omitting those terms which contain a different number of core creation and destruction operators $a_c^\dagger$ and a_c. This has been discussed in great detail in Ref. 24, and we shall only give a short review here.

Assuming that the core orbitals are strongly localized at the atomic sites, the probability for a

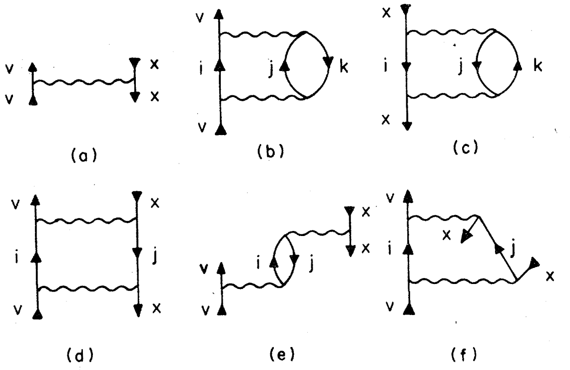

FIG. 3. Feynman diagrams needed for the calculation of the excitation energy up to second order.

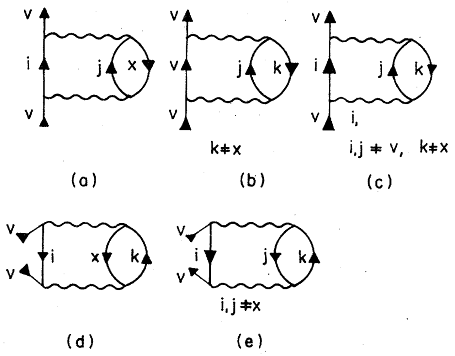

FIG. 4. Diagrammatic decomposition of Fig. 3(b) according to Eq. (23).

hole propagation from ϕ_{c1} to ϕ_{c2} is very low even in the case of nearly degenerate orbitals. In case of degenerate orbitals one can make a linear combination of the core orbitals and transform into a basis of strongly localized orbitals. Thus we can use a Hamiltonian with only a single core hole present. This Hamiltonian reads[24]

$$H_{cv} = H_c + H_v + W_{cv} + F_{cv} . \qquad (24)$$

H_c contains only core interactions and is given by

$$H_c = \epsilon_c(\hat{n}_c + \hat{n}_{\bar{c}}) + V_{cccc}\hat{n}_c\hat{n}_{\bar{c}} + v_{cc}(\hat{n}_c + \hat{n}_{\bar{c}}) , \qquad (25a)$$

where $\hat{n}_c = a_c^\dagger a_c$ is the core number operator of α spin and $\hat{n}_{\bar{c}}$ denotes the same with β spin. The valence interaction term reads

$$H_v = \sum_i \epsilon_i a_i^\dagger a_i - \sum_{ij}\left(\sum_k V_{ik[jk]} n_k\right) a_i^\dagger a_j + \tfrac{1}{2}\sum_{ijkl} V_{ijkl} a_i^\dagger a_j^\dagger a_l a_k , \qquad (25b)$$

where the indices i, j, k, and l do not include the core index any more. The operator

$$F_{cv} = \left(-\sum_{ij} V_{ic\bar{c}j} a_i^\dagger a_j\right) a_c^\dagger a_{\bar{c}} + \text{H.c.} \qquad (25c)$$

does not preserve the spin of the core electrons and is referred to as the spin-flip term. If F_{cv} is neglected, the eigenfunctions of H_{cv} are no longer eigenfunctions of S^2. The last term W_{cv} contains the remaining (spin-preserving) core-valence interaction

$$W_{cv} = -(1 - \hat{n}_c)\sum_{ij} V_{ic[jc]} a_i^\dagger a_j + (c \leftrightarrow \bar{c}) . \qquad (25d)$$

Because the spin-flip term contains only exchange Coulomb integrals between core and valence orbitals it is small and can be neglected in many cases of interest. The effect of the spin-flip term can be incorporated subsequently in the calculation by using the eigenfunctions of the Hamiltonian $H_{cv} = H_c + H_v + W_{cv}$ and diagonalizing matrices of very low dimensions including only those nearly degenerate states which are coupled via F_{cv}. In the following analysis we neglect the spin-flip term F_{cv}.

B. The Bethe-Salpeter equation

A calculation of the core polarization propagator can be performed, at least theoretically, by using the Hamiltonian H_{cv} of Eq. (24) and solving the Bethe-Salpeter equation (9). In Ref. 24 it is shown that the Hamiltonian H_{cv} leads to a conservation of the core index at every vertex (interaction line). This means that the core Green's function and the core-polarization propagator are both diagonal in the core index. Incorporating this result into the Bethe-Salpeter equation (9) we obtain for the core-valence excitation the following equation:

$$\begin{aligned}(-i)\Pi_{icjc}(t, -\tau) = {} & iG_{ij}(t)iG_{cc}(-\tau) \\ & + \sum_{\alpha,\beta}\int_{-\infty}^{+\infty} dt_1 dt_3 \int_0^{\tau} dt_4 \int_{\tau_4}^{\tau} dt_2\, iG_{i\alpha}(t - t_1) iG_{cc}(t_2 - \tau) \\ & \times iK_{\alpha c\beta c}(t_1 - t_3, t_4 - t_2, t_1 - t_2)(-i)\Pi_{\beta cjc}(t_3, -t_4) . \end{aligned} \qquad (26)$$

It can be seen that the integration limits which involve the core interactions (t_2 and t_4) are restricted to times between 0 and τ while the other integration limits (t_1 and t_3) have no such restriction. The illustration of Eq. (26) can be obtained from Fig. 2 by incorporating the conservation of the core index. Thus, the only diagrams contributing in nth order to Π_{icjc} are those which contain $(n+1)$ or less successive core lines iG_c^0. No additional core lines are allowed. This is valid for both linked and unlinked diagrams.

Equation (26) is certainly very difficult to solve because it is still a multidimensional integral equation in t space. If we use again approximation (11) many terms vanish, since the valence interactions carrying an external index (α or β) are restricted to the same time interval as the core interactions. In this case a Fourier transformation to an algebraic equation in ω space is possible and we obtain

$$\Pi_{icjc}(\omega) = \Pi_{icjc}^0(\omega) + \sum_{\alpha,\beta} \Pi_{ic\alpha c}^0(\omega) K_{\alpha c\beta c}(\omega) \Pi_{\beta cjc}(\omega) . \qquad (27)$$

If we substitute $K_{\alpha c\beta c}(\omega)$ in Eq. (27) by its first-order approximation $-V_{\alpha c[\beta c]}$ and replace $\Pi_{icjc}^0(\omega)$ by the noninteracting case of Eq. (4) the Tamm-Dancoff Approximation (TDA) is again obtained. The (TDA) eigenvalue equation is Hermitian and reads

$$(\omega - \epsilon_i + \epsilon_c)\bar{n}_i C_{ic} + \sum_\alpha V_{ic[\alpha c]}\bar{n}_i \bar{n}_\alpha C_{\alpha c} = 0 , \qquad (28)$$

where i and α refer to particles. The dimension of the corresponding matrix is very small and equals the number of unoccupied HF orbitals. Because the core index always refers to a hole it is obvious that the time ordering of the corresponding diagrams cannot be reversed. Thus, the random-phase approximation is identical to the Tamm-Dancoff approximation.

In Eq. (28) only a part of the valence relaxation is considered. The use of G lines instead of G^0 lines especially for the core Green's function in Π^0 would be an essential step in obtaining a more sophisticated approximation. The exact core Green's function takes into account the important term due to the change of relaxation of the valence electrons in the presence of a core hole.

C. Factorization theorem

A theoretical treatment of core-valence excitations via the simplified Bethe-Salpeter Eqs. (27) and (28) is not quite satisfactory because of the above-mentioned neglection of terms. We, therefore, return to the more general Bethe-Salpeter equation (26). In the case of core-valence excitations it can be shown by using the Hamiltonian H_{cv} of Eq. (24) without the spin-flip term that the polarization propagator satisfies an important factorization theorem (for an analytical proof of this theorem, see Appendix A)

$$(-i)\Pi_{i\text{c}j\text{c}}(t,-\tau)=i\rho_{ij}(t;\tau)iG_{\text{cc}}(-\tau)\,, \tag{29}$$

where $G_{\text{cc}}(-\tau)$ is the core Green's function and $\rho_{ij}(t;\tau)$ is a valence Green's function with a time-dependent core potential. τ is a parameter for this function and corresponds to the core-hole "lifetime" which should not be confused with the natural lifetime.

The factorization theorem (29) states that the core-valence excitation process can be decomposed into a product of two independent processes, namely a core ionization and a valence attachment in the field of the core potential. This decomposition is done at the cost of introducing an additional time-dependent potential into the Hamiltonian describing the valence attachment. In addition to the usual valence interaction potential between the electrons we have a time-dependent core potential which reads

$$V(t)=V_1\Theta(\tau-t)\Theta(t)\,, \tag{30}$$

where V_1 is just the Coulomb potential plus exchange of the core hole

$$V_1=-\sum_{k,l}V_{k\text{c}[l\text{c}]}(a_k^\dagger a_l-n_k\delta_{kl})\,. \tag{31}$$

The physical interpretation of the factorization theorem can now be expressed as follows. At time 0 a core hole c and a valence particle j are simultaneously created. The core hole propagates through the system independently until it is annihilated at time τ. This process is described by the diagonal core Green's function $G_{\text{cc}}(-\tau)$. The valence particle j, where j can refer to a HF hole or particle, propagates through the system in the field of the core potential (31). This potential is turned on between the times 0 and τ while the valence particle j propagates between 0 and t. Thus, the valence attachment process depends on two different times t and τ, whereby the latter has the meaning of a parameter accounting for the change in the interaction term while the core hole is present. The physical information of interest are the core-valence excitation energies and the corresponding intensities. These are contained in the core polarization propagator $\Pi_{i\text{c}j\text{c}}(t)$ which is given by

$$\begin{aligned}\Pi_{i\text{c}j\text{c}}(t)&=\lim_{\tau\to t}\Pi_{i\text{c}j\text{c}}(t,-\tau)\\&=(-i)\rho_{ij}(t)G_{\text{cc}}(-t)\,,\end{aligned} \tag{32}$$

where

$$\rho_{ij}(t)=\lim_{\tau\to t}\rho_{ij}(t;\tau)\,.$$

For the description of the core-valence excitations we create a core-hole valence-particle pair at time 0 and annihilate it again at time t. This is equivalent to the propagation of a density disturbance from one point to another. A Fourier transformation of Eq. (32) can formally be done,

$$\Pi_{i\text{c}j\text{c}}(\omega)=(-i)\int\frac{d\omega'}{2\pi}\rho_{ij}(\omega')G_{\text{cc}}(\omega'-\omega)\,, \tag{33}$$

where $\rho_{ij}(\omega)$ is the Fourier transform of $\rho_{ij}(t)$,

$$\rho_{ij}(\omega)=\int dt\,e^{i\omega t}\rho_{ij}(t)\,. \tag{34}$$

In ω space the core polarization propagator is determined by a convolution of the valence Green's function $\rho_{ij}(\omega)$ with the core Green's function $G_{\text{cc}}(\omega)$. It is important to notice that $\rho_{ij}(\omega)$ has in general a very complicated spectral representation. This becomes clear by looking at Appendix C [see Eq. (C12)], where some properties of $\rho_{ij}(t;\tau)$ are derived. More useful, however, is a glance at the example of Sec. IV where a Lehmann representation for $\rho(t)$ has been derived explicitly, see Eq. (72). Even in this simple three-level model, $\rho(\omega)$ has infinitely many poles and the convolution of the two one-particle Green's functions to $\Pi(\omega)$ leads to a cancellation of almost all poles.

The core Green's function $G_{\text{cc}}(-\tau)$ appearing in the factorization theorem (29) has been discussed in Ref. 24. Starting from the Hamiltonian H_{cv} (29) without the spin-flip term F_{cv} a linked cluster theorem can be proved

$$G_{\text{cc}}(-\tau)=G_{\text{cc}}^0(-\tau)e^{C(-\tau)}=i\Theta(\tau)e^{i\epsilon_{\text{c}}\tau}e^{C(-\tau)}\,. \tag{35}$$

$C(-\tau)$ is the sum of all linked topologically nonequivalent diagrams containing at least one core interaction point. In nth order the diagrams can be drawn from $n_1(\geq 1)$ interaction points and $n_2 = n - n_1$ wiggly lines connected via $(2n - n_1)iG^0$ (valence) lines. The wiggly lines and the interaction points must be treated differently. Whereas the time level of the core interaction points is restricted to the time interval $(0, \tau)$, the time level of a wiggly line is, as usual, between $-\infty$ and $+\infty$.

In Eq. (29) we have also introduced the valence Green's function $\rho_{ij}(t;\tau)$ with a time-dependent core potential. This function is rather unusual and it is, therefore, necessary to discuss it in detail. A Heisenberg representation of $\rho_{ij}(t;\tau)$ has been derived in Appendix B

$$i\rho_{ij}(t;\tau) = \frac{\langle \Psi_0^{N_v}(\tau) | T[a_i(t) a_j^\dagger] | \Psi_0^{N_v}\rangle}{\langle \Psi_0^{N_v}(\tau) | \Psi_0^{N_v}\rangle} \,. \tag{36}$$

$|\Psi_0^{N_v}\rangle$ is the exact valence ground state developed from the unperturbed ground state without the time-dependent core potential being present. $|\Psi_0^{N_v}(\tau)\rangle$ is the corresponding state developed in the field of the time-dependent core potential. The operators in the Heisenberg picture are defined by

$$a_i(t) = U_\tau^{-1}(t) a_i U_\tau(t) \,, \tag{37}$$

where $U_\tau(t)$ is the general time-development operator which in the special case of a time-independent Hamiltonian is identical to e^{-iHt}.

Equation (36) can be compared to the usual definition of a one-particle valence Green's function[10]

$$iG_{ij}(t) = \frac{\langle \Psi_0^{N_v} | T[a_i(t) a_j^\dagger] | \Psi_0^{N_v}\rangle}{\langle \Psi_0^{N_v} | \Psi_0^{N_v}\rangle} \,. \tag{38}$$

Normalizing the ground state $\langle \Psi_0^{N_v} | \Psi_0^{N_v}\rangle = 1$ and considering only the time ordering $t \geq 0$ we obtain

$$iG_{ij}(t) = \langle \Psi_0^{N_v} | e^{iHt} a_i e^{-iHt} a_j^\dagger | \Psi_0^{N_v}\rangle \,. \tag{39}$$

This expression can be interpreted in the Schrödinger picture as follows.[12] Starting from the HF ground state $|\Phi_0^{N_v}\rangle$ at $t' = -\infty$ the state propagates until $t' = 0$ with a time-development operator including only interactions between the valence electrons. In this way we obtain the ground state $|\Psi_0^{N_v}\rangle$. Next we create a particle in orbital ϕ_j. The new state propagates with the time-development operator e^{-iHt} until t

$$|A\rangle = e^{-iHt} a_j^\dagger | \Psi_0^{N_v}\rangle \,.$$

On the other side, the HF ground state $|\Phi_0^{N_v}\rangle$ can propagate from $t' = +\infty$ until $t' = 0$ yielding again the ground state $|\Psi_0^{N_v}\rangle$. The system propagates then with e^{-iHt} until t followed by the creation of a particle in orbital ϕ_i

$$|B\rangle = a_i^\dagger e^{-iHt} | \Psi_0^{N_v}\rangle \,.$$

The Green's function $iG_{ij}(t)$ is identical to $\langle B | A\rangle$ which is just the probability amplitude that the state of the system at t, when a particle in ϕ_j was added to the ground state at 0, is the state with one particle in ϕ_i added to the ground state at time t.[12] The other time ordering $(t \leq 0)$ can be interpreted in the same way.

In complete analogy we can discuss the Green's function $\rho_{ij}(t;\tau)$ of Eq. (36). Starting from the HF ground state $|\Phi_0^{N_v}\rangle$ at $t' = -\infty$ the state propagates until $t' = 0$ with the time-development operator including, in addition to the interactions between the valence electrons, the time-dependent core potential of Eqs. (30) and (31). During this time interval, however, the core-interaction potential is not switched on and thus we obtain the valence ground state $|\Psi_0^{N_v}\rangle$ again. Then a particle in orbital ϕ_j is added to the system. This state propagates with the general time-devleopment operator $U_\tau(t)$ until t

$$|A\rangle = U_\tau(t) a_j^\dagger | \Psi_0^{N_v}\rangle \,.$$

On the other side, the HF ground state $|\Phi_0^{N_v}\rangle$ can propagate from $t' = +\infty$ until $t' = 0$ where the time-dependent core potential is switched on between the times 0 and τ yielding the ground state $|\Psi_0^{N_v}(\tau)\rangle$. The system propagates with $U_\tau(t)$ until t and then a particle is created in orbital ϕ_i

$$|B\rangle = a_i^\dagger U_\tau(t) | \Psi_0^{N_v}(\tau)\rangle \,.$$

The Green's function $i\rho_{ij}(t;\tau)$ is identical to $\langle B | A\rangle$ which can thus be interpreted analogously to $iG_{ij}(t)$ as a probability amplitude.[12]

It is also useful to interpret the valence Green's function $\rho_{ij}(t;\tau)$ in the interaction picture [Eq. (A18) of Appendix A]

$$i\rho_{ij}(t;\tau) = \frac{\langle \Phi_0^{N_v} | T[\tilde{U}_\tau(+\infty, -\infty) \bar{a}_i(t) \bar{a}_j^\dagger] | \Phi_0^{N_v}\rangle}{\langle \Phi_0^{N_v} | \tilde{U}_\tau(+\infty, -\infty) | \Phi_0^{N_v}\rangle} \,, \tag{40}$$

where

$$\tilde{U}_\tau(+\infty, -\infty) = \sum_n \frac{(-i)^n}{n!} \times \int_{-\infty}^{+\infty} dt_1 \cdots \int_{-\infty}^{+\infty} dt_n T[\bar{V}(t_1) \cdots \bar{V}(t_n)] \tag{41}$$

is the time-development operator which includes, in addition to the usual interaction potential between the valence electrons, the time-dependent core potential of Eqs. (30) and (31). Obviously all theorems which have been proven for the usual time-development operator without an explicitly time-dependent potential remain true for the general operator $\tilde{U}_\tau(T_2, T_1)$ (Ref. 10) especially the Gell-Mann and Low theorem and Wick's theorem. Hence it follows that $\rho_{ij}(t;\tau)$ is a one-particle

Green's functions which can be interpreted in terms of diagrams. In Fig. 1 we have introduced the required graphical symbols. Two types of interactions can appear, namely the usual valence interaction wiggle $V_{ij[kl]}$ and the core-interaction point $V_{ic[jc]}$. Starting from the noninteracting HF valence ground state $|\Phi_0^{N_v}\rangle$ at $t'=-\infty$ the system can perform all kinds of interactions $V_{ij[kl]}$ between the valence electrons during its propagation until $t'=0$. Then a particle is created in ϕ_j and between 0 and τ both types of interactions $V_{ij[kl]}$ and $V_{ic[jc]}$ can appear, i.e., during this time interval the system contains the additional core potential. At $t'=t$, a particle is annihilated in ϕ_i and from $t'=\tau$ on again only the valence interactions $V_{ij[kl]}$ are permitted. In the limes $t'=+\infty$ the noninteracting ground state $|\Phi_0^{N_v}\rangle$ is again obtained. Thus it is clear that although the time dependence of the core potential leads to a mathematically complicated theory for the valence Green's function $\rho_{ij}(t;\tau)$ the diagrammatic interpretation remains both simple and illustrative.

D. Diagrammatic analysis of $\rho(t;\tau)$

In Sec. IIIC we have introduced the valence Green's function $\rho_{ii}(t;\tau)$ with a time-dependent core potential. The knowledge of this Green's function together with the core Green's function $G_{cc}(-\tau)$ enables us to calculate the core-valence excitation spectrum. It is, therefore, important to derive an expression which allows us to calculate the valence Green's function $\rho_{ij}(t;\tau)$ systematically. From Eq. (36) it is clear that $\rho_{ij}(t;\tau)$ can be written as

$$i\rho_{ij}(t;\tau)=\langle\Phi_0^{N_v}|T[\tilde{U}_\tau(+\infty,-\infty)\bar{a}_i(t)\bar{a}_j^\dagger]\,|\Phi_0^{N_v}\rangle_L\,, \tag{42}$$

where the index L implies that we have to consider only linked terms (linked cluster theorem[10]). Equation (42) is readily visualized as a perturbational expansion of $\rho_{ij}(t;\tau)$,

$$i\rho_{ij}(t;\tau)=\sum_{n=0}^{\infty}\frac{(-i)^n}{n!}\int_{-\infty}^{+\infty}dt_1\cdots\int_{-\infty}^{+\infty}dt_n\langle\Phi_0^{N_v}|T[\bar{V}(t_1)\cdots\bar{V}(t_n)\bar{a}_i(t)\bar{a}_j^\dagger]\,|\Phi_0^{N_v}\rangle_L\,, \tag{43}$$

where $\bar{V}(t_i)$ includes, in addition to the usual interaction potential between the valence electrons, the time-dependent core potential of Eqs. (30) and (31). Wick's theorem enables us to evaluate the exact valence Green's function $\rho_{ij}(t;\tau)$ as a perturbation expression involving only wholly contracted operators $\bar{a}_m(t),\bar{a}_n^\dagger(t)$ in the interaction picture. Since our potential is explicitly time-dependent, we have to pay attention to the integration limits. Although Eq. (43) allows us to calculate the various contributions to $\rho_{ij}(t;\tau)$ in each order of the perturbation theory in a straightforward way it is much easier to use a diagrammatic approach. The diagrams of $\rho_{ij}(t;\tau)$ are readily obtained from the diagrams of $\Pi_{icjc}(t,-\tau)$ by projecting out the core Green's function $G_{cc}(-\tau)$, i.e., via the use of the factorization theorem (29). The diagrammatic perturbation expansion of $\rho_{ij}(t;\tau)$ up to second order is depicted in Fig. 5. The diagrams are not time ordered. It is important to note that in a calculation of $\rho_{ij}(t;\tau)$ via a perturbation expansion, where we calculate the contribution of each diagram individually, we may *a priori* substitute τ by t in each diagram. The core-hole "lifetime" is then equal to t.

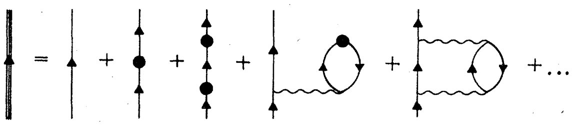

FIG. 5. Diagrammatic expansion of $\rho(t;\tau)$.

Obviously the function $\rho_{ij}(t;\tau)$ consists in nth order of all linked diagrams with $n_1(\geqslant 0)$ core-interaction points and $n_2=n-n_1(\geqslant 0)$ valence interaction wiggles starting with a G^0 line and ending with a G^0 line. We may thus write

$$\rho_{ij}(t;\tau)=G_{ij}^0(t)+\sum_{\alpha,\beta}\int dt_1dt_2G_{i\alpha}^0(t-t_1)\times\hat{\Sigma}_{\alpha\beta}(t_1,t_2;\tau)G_{\beta j}^0(t_2)\,. \tag{44}$$

The self-energy part $\hat{\Sigma}$ introduced in this way contains all the diagrams of ρ with the two external G^0 lines removed. As an illustration we show three examples of time-ordered diagrams of $\hat{\Sigma}$ in Fig. 6. Figures 6(a), 6(b), and 6(c) result

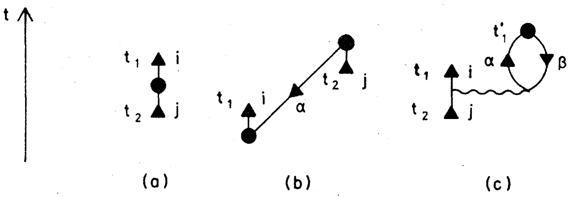

(a) (b) (c)

FIG. 6. Three time-ordered diagrams of $\hat{\Sigma}$. The time axis is shown on the left.

from the second, third, and fourth diagram shown on the right-hand side of the equation in Fig. 5, respectively. Each of the diagrams Fig. 6(b) and 6(c) is, however, only one of the two possible time-ordered diagrams obtainable from a non-time-ordered diagram of second order.

Using Fig. 1 and the corresponding explication in Sec. IIA a translation of these diagrams is easily performed. The first-order diagram, Fig. 6(a), is equal to

$$iV_{ic[jc]}\Theta(\tau-t_1)\Theta(t_1)\delta(t_1-t_2)\,.$$

Figure 6(b) yields the following contribution:

$$\sum_{\alpha,\beta} iV_{ic[\alpha c]}iG^0_{\alpha\alpha}(t_1-t_2)iV_{\alpha c[jc]}$$
$$\times\,\Theta(\tau-t_1)\Theta(t_1)\Theta(\tau-t_2)\Theta(t_2-t_1)\,.$$

Finally we obtain for Fig. 6(c),

$$\sum_{\alpha,\beta}(-i)V_{i\alpha[j\beta]}iV_{\alpha c[\beta c]}\delta(t_1-t_2)\int dt_1' iG^0_{\alpha\alpha}(t_1'-t_1)iG^0_{\beta\beta}(t_1-t_1')\Theta(\tau-t_1')\Theta(t_1')\Theta(t_1'-t_1)\,.$$

It is clear that the time restriction of the core potential complicates the problem of evaluating the diagrams. Analogously to the usual textbook procedure for time-independent potentials we can derive a Dyson equation also for the Green's function ρ_{ij}. We first define the proper (or irreducible) self-energy part Σ by the sum of all those diagrams of $\hat{\Sigma}$ that cannot be separated into two pieces by cutting a single *free* Green's function line. For example, Figs. 6(a) and 6(c) contain irreducible diagrams and consequently belong to Σ, while Fig. 6(b) is reducible and does not belong to Σ. It follows from these definitions that the self-energy $\hat{\Sigma}$ consists of the sum of all possible repetitions of the proper self-energy Σ (Ref. 10)

$$\hat{\Sigma}_{ij}(t,t';\tau)=\Sigma_{ij}(t,t';\tau)+\sum_{\alpha,\beta}\int dt_1dt_2\Sigma_{i\alpha}(t,t_1;\tau)G^0_{\alpha\beta}(t_1-t_2)\Sigma_{\beta j}(t_2,t';\tau)+\cdots\,. \tag{45}$$

Inserting this into Eq. (44) we finally obtain for $\rho_{ij}(t;\tau)$ the following Dyson equation:

$$\rho_{ij}(t;\tau)=G^0_{ij}(t)+\sum_{\alpha,\beta}\int dt_1dt_2G^0_{i\alpha}(t-t_1)\Sigma_{\alpha\beta}(t_1,t_2;\tau)\rho_{\beta j}(t_2;\tau)\,. \tag{46}$$

This is an integral equation for the valence Green's function $\rho_{ij}(t;\tau)$ where we have to bear in mind that, in general, the irreducible self-energy Σ depends in a complicated way on the core hole "lifetime". The time dependence of Σ does not only occur through the time difference t_1-t_2, but involves also combinations of t_1 and t_2 with τ. In Eq. (46), the limit $\tau\rightarrow t$ can only be performed after the calculation of $\rho_{ij}(t;\tau)$. In the field of the external core hole potential, it is not possible to convert Eq. (46) into an algebraic equation in ω space as can be done for the commonly used Dyson equation.

The irreducible self-energy can be decomposed according to

$$\Sigma_{ij}(t,t';\tau)=\Sigma^K_{ij}(t,t';\tau)+\Sigma^V_{ij}(t-t')\,, \tag{47}$$

where Σ^V contains all the diagrams of Σ without any core-interaction points and Σ^K contains the diagrams with at least one core interaction. For example, Figs. 6(a) and 6(c) belong to Σ^K and Fig. 3(b) belongs to Σ^v. Obviously Σ^V depends only on the time difference $t-t'$. It can now be shown that Eq. (46) is equivalent to the pair of equations

$$G_{ij}(t)=G^0_{ij}(t)+\sum_{\alpha,\beta}\int dt_1dt_2G^0_{i\alpha}(t-t_1)\Sigma^V_{\alpha\beta}(t_1-t_2)G_{\beta j}(t_2)\,, \tag{48a}$$

$$\rho_{ij}(t;\tau)=G_{ij}(t)+\sum_{\alpha,\beta}\int dt_1dt_2G_{i\alpha}(t-t_1)\Sigma^K_{\alpha\beta}(t_1,t_2;\tau)\rho_{\beta j}(t_2;\tau)\,, \tag{48b}$$

implying that we may determine $\rho_{ij}(t;\tau)$ in two steps. At first the Green's function $G_{ij}(t)$ is evaluated. This is just the usual Green's function involving only the valence electrons and their interactions. An actual calculation of $G_{ij}(t)$ may be performed in ω space. Then $\rho_{ij}(t;\tau)$ is evaluated in t space via Eq. (48b).

There is an alternative decomposition of Σ, namely,

$$\Sigma_{ij}(t,t';\tau)=\Sigma^C_{ij}(t,t';\tau)+\Sigma^R_{ij}(t,t';\tau)\,. \tag{49}$$

Σ^C is that part of the irreducible self-energy containing all the diagrams exhibiting core interaction points only, while Σ^R contains the rest. In this case the Dyson equation (46) is equivalent to the following equations:

$$\rho^0_{ij}(t;\tau)=G^0_{ij}(t)+\sum_{\alpha,\beta}\int dt_1dt_2G^0_{i\alpha}(t-t_1)\Sigma^C_{\alpha\beta}(t_1,t_2;\tau)\rho^0_{\beta j}(t_2;\tau)\,, \tag{50a}$$

$$\rho_{ij}(t;\tau)=\rho^0_{ij}(t;\tau)+\sum_{\alpha,\beta}\int dt_1 dt_2\,\rho^0_{i\alpha}(t-t_1;\tau)\Sigma^R_{\alpha\beta}(t_1,t_2;\tau)\rho_{\beta j}(t_2;\tau)\,. \tag{50b}$$

In Eq. (50a) we have introduced $\rho^0_{ij}(t;\tau)$ containing all diagrams of $\rho_{ij}(t;\tau)$ without any valence interaction wiggle. $\rho^0_{ij}(t;\tau)$ has already the correct analytical time structure exhibited by the exact function $\rho_{ij}(t;\tau)$. The diagrams of the self-energy part Σ^R can be visualized as diagrams containing only valence interaction wiggles, but the Green's function lines connecting these wiggles have to be interpreted as ρ^0 lines. Thus, we obtain the diagrams of Σ^R from the diagrams of Σ^V by substituting all G^0 lines by ρ^0 lines.

It is clear that all equations for $\rho_{ij}(t;\tau)$ are very complicated to solve at least for most realistic physical systems. To illustrate the principle of working with these equations we consider here a simple case and substitute Σ_{ij} by its first-order contribution $-V_{i\mathrm{c}[j\mathrm{c}]}$, where i,j refer to particle indices (for another example, see also Sec. IV). In this case we can obtain for Σ_{ij} an equation depending only on t by using Eq. (46) and performing $\tau\to t$ first:

$$\rho_{ij}(t)=G^0_{ij}(t)-\sum_{\alpha,\beta}\int_0^t dt_1\,G^0_{i\alpha}(t-t_1)V_{\alpha\mathrm{c}[\beta\mathrm{c}]}\rho_{\beta j}(t_1)\,. \tag{51}$$

This equation can easily be transformed to ω space and finally leads to the following set of Hermitian eigenvalue equations for the poles and residues of ρ

$$(\omega-\epsilon_i)\bar{n}_iC_i+\sum_\alpha V_{i\mathrm{c}[\alpha\mathrm{c}]}\bar{n}_i\bar{n}_\alpha C_\alpha=0\,. \tag{52}$$

This low-level result reminds us of the TDA equation (28). Ths core-valence excitation energies of Eq. (28) are just the electron-attachment energies obtained as eigenvalues of Eq. (52) shifted by the core orbital energy ϵ_c.

E. Analysis of the core-valence excitation energy

The core-valence excitation energy is a special case of the general excitation energy in Sec. II B and it is obtained by using the Hamiltonian H_cv of Eq. (24) instead of the full Hamiltonian (2). Performing the same procedure as has been described in Sec. II B we obtain for the ΔSCF energy up to second order the following expression:

$$\Delta E^{\mathrm{SCF}}_{\mathrm{c}\to\mathrm{v}}=\epsilon_\mathrm{v}-\epsilon_\mathrm{c}-V_{\mathrm{cv}[\mathrm{cv}]}+\sum_{i,j\neq\mathrm{c}}\frac{|V_{i\mathrm{v}[j\mathrm{v}]}|^2}{\epsilon_j-\epsilon_i}\bar{n}_in_j+\sum_{i\neq\mathrm{v},j}\frac{|V_{i\mathrm{c}[j\mathrm{c}]}|^2}{\epsilon_j-\epsilon_i}\bar{n}_in_j$$
$$+\sum_{i\neq\mathrm{v}}\frac{|V_{\mathrm{vc}[i\mathrm{c}]}|^2}{\epsilon_\mathrm{v}-\epsilon_i}\bar{n}_i-2\sum_{ij}\frac{V_{i\mathrm{c}[j\mathrm{c}]}V_{j\mathrm{v}[i\mathrm{v}]}}{\epsilon_j-\epsilon_i}\bar{n}_in_j\,. \tag{53}$$

Correspondingly the correlation energy is given by

$$\Delta E^{C}_{\mathrm{c}\to\mathrm{v}}=\tfrac{1}{2}\sum_{ikl}{}'\frac{|V_{\mathrm{v}j[kl]}|^2}{\epsilon_\mathrm{v}+\epsilon_j-\epsilon_k-\epsilon_l}n_j\bar{n}_k\bar{n}_l$$
$$+\tfrac{1}{2}\sum_{jkl}{}'\frac{|V_{\mathrm{v}j[kl]}|^2}{\epsilon_\mathrm{v}+\epsilon_j-\epsilon_k-\epsilon_l}\bar{n}_jn_kn_l\,, \tag{54}$$

where the prime indicates that the summation excludes the core index c and the valence index v. The total core-valence excitation energy is again given by

$$\Delta E_{\mathrm{c}\to\mathrm{v}}=\Delta E^{\mathrm{SCF}}_{\mathrm{c}\to\mathrm{v}}+\Delta E^{C}_{\mathrm{c}\to\mathrm{v}}\,.$$

These results can also be obtained from the general expressions for the excitation energies Eqs. (18) and (20) by setting $x\equiv\mathrm{c}$ and taking into account the core-valence separability. If we simply set $x\equiv\mathrm{c}$ in Eqs. (18) and (20), which corresponds to the use of the full Hamiltonian (2), we obtain the exact second-order core-valence excitation energies. Then it is easily shown that the only relaxation term which is neglected in Eq. (53) is given by

$$\sum_{j\neq c}\frac{|V_{j\mathrm{v}[\mathrm{cv}]}|^2}{\epsilon_j-\epsilon_\mathrm{c}}n_j\,.$$

The matrix elements $V_{j\mathrm{v}[\mathrm{cv}]}$ appearing in the numerator of this expression are small due to the weak overlap of the valence orbitals with the core orbital. In addition, the denominator is always rather large because of the great energetic difference between the valence orbital j and the core orbital c. For the correlation energy it can be seen that the use of H_cv(24) leads to the neglect of the following terms

$$\tfrac{1}{2}\sum_{ijk}{}'\frac{|V_{ij[k\mathrm{c}]}|^2}{\epsilon_i+\epsilon_j-\epsilon_k-\epsilon_c}(n_i\bar{n}_j\bar{n}_k+\bar{n}_in_jn_k)$$
$$+\sum_{ik}{}'\frac{|V_{iv[\mathrm{c}k]}|^2}{\epsilon_i+\epsilon_\mathrm{v}-\epsilon_\mathrm{c}-\epsilon_k}(n_i\bar{n}_k+\bar{n}_in_k)\,,$$

where the argument for neglecting these sums is the same as above. Therefore, we can draw the following conclusion: If H_{cv} of Eq. (24) is used instead of the full Hamiltonian (2) then several terms are neglected. These terms yield very small contributions reflecting the accuracy of H_{cv} in describing core-valence excitation processes.

A diagrammatic analysis can easily be performed by using the same arguments as in Sec. II B. In this way one can relate the analytical expressions to simple physical processes. All time-ordered diagrams contributing to $\Delta E_{c\to v}$ up to second order are shown in Fig. 7. They can be interpreted as follows. Figure 7(a) represents the first-order core-valence interaction $V_{cv[cv]}$ containing the Coulomb interaction between the occupied valence-orbital v and the nonoccupied core-orbital plus the corresponding exchange term. This contribution shifts the zeroth-order excitation energy $\epsilon_v - \epsilon_c$ to lower energies. In first order the particles and holes remain "static" which means they remain in their unperturbed stationary states (frozen orbitals). But in reality their motion is perturbed by the ionized or attached electron. Thus they act in a "dynamic" rather than a static way, i.e., in a time-dependent fashion. The simplest processes showing this effect appear in second order.

Let us consider the neutral system and create a core hole. Then the orbitals reorganize in the field of the core hole via particle-hole excitations $(j\to i)$. This process corresponds to Figs. 7(c) and 7(d). Next we attach an additional electron to the orbital v in the neutral system. Then this orbital is occupied and the other orbitals relax in the presence of this electron via particle-hole excitations $(j\neq c\to i)$. This reorganization is described by Fig. 7(b) and is equal to the first sum of Eq. (53). The term with $j=c$ is missing due to the choice of our Hamiltonian. Next we consider the case where the core electron c is excited to the valence-orbital v. This means the core-hole and the valence-particle are simultaneously present in the system. Figures 7(e)–7(h) correspond to this process. Due to the presence of Fig. 7(e) the relaxation of the valence-orbital v is subtracted again. Then the reorganization of all orbitals except v in the presence of the core-hole [Fig. 7(c)] is equal to the second sum of Eq. (53). The relaxation of the valence-orbital v in the presence of the core hole is incorporated in our calculation by Fig. 7(f) describing the simultaneous propagation of the particle v and the hole c. v and c interact with one another leading to excitation $v\to i\neq v$. This means the valence-orbital v does not relax as an occupied orbital because the two contributions of Figs. 7(d) and 7(e) cancel. The orbital v relaxes, however, as an unoccupied orbital [Fig. 7(f)] and the corresponding analytical expression is given by the third sum of Eq. (53). It should be noted that the choice of the Hamiltonian H of Eq. (2) instead of H_{cv} of Eq. (24) leads to completely analogous arguments for the relaxation of the core-orbital c.

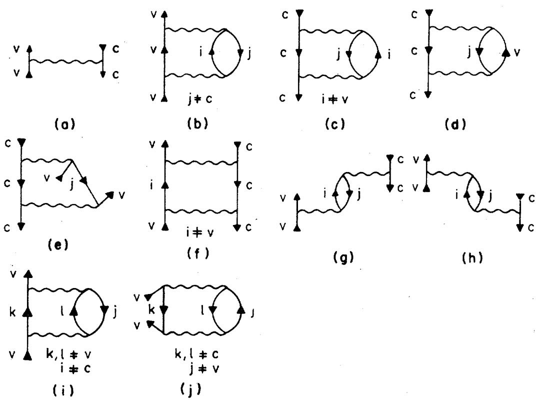

FIG. 7. Time-ordered diagrams of the core-valence excitation energy $\Delta E_{c\to v}$. (a)–(h) represent relaxation terms and (i) and (j) represent correlation terms.

In addition to the reorganization of the orbitals in the presence of the core-hole or the valence-particle, respectively, we have an interference term describing the orbital relaxation when a core-hole c and a valence-particle v are simultaneously present. While in Fig. 7(b) the particle-hole pair is both created or annihilated by the interaction with the electron in orbital v leading to a term which is quadratic in the valence interaction (V_v^2), and in Fig. 7(c) this happens via the core interaction (V_c^2) there is an additional interference term $(V_v V_c)$ represented by Fig. 7(g) and 7(h). This can be visualized as follows: In Fig. 7(g) an electron is excited from orbital j to orbital i by the interaction with the electron in the valence-orbital v (V_v). This particle-hole pair propagates through the system until it is annihilated by the interaction with the core hole (V_c). Analogously, in Fig. 7(h) the particle-hole pair is created by the core potential (V_c) and destructed by the interaction with the electron in orbital v (V_v). Both diagrams correspond to the same analytical expression. The interference term is given by the last sum of Eq. (53). Hence, it is clear that the interaction potential describing the orbital relaxation is given by the sum of the valence interaction V_v and the core interaction V_c.

In addition to the above-discussed reorganization terms there are two terms accounting for the exchange of the correlation energy illustrated by

Figs. 7(i) and 7(j). Owing to the occupation of the orbital v there is a term which takes into account the additional pair correlation energies. It is represented by Fig. 7(j) and is equal to the second sum of Eq. (54). Hence, in the case of core-valence excitations the lowest order correction to the ground-state correlation energy occurs in second order while for core ionizations it occurs in third order. In addition, there is a term accounting for the changes in the remaining pair correlations due to reorganizations (pair relaxation). This process corresponds to Fig. 7(i). The analytical expression is given by the first sum of Eq. (54). Finally it should be mentioned that the approximation of Eq. (11) is not applicable because Figs. 7(e), 7(g), and 7(h) yield a wrong contribution in this case.

A general decomposition of higher order diagrams can be performed using the factorization theorem for the core polarization propagator. The one-particle Green's function G consists of an unperturbed term G^0, a relaxation term R, and a correlation term K,

$$G = G^0 + R + K .$$

According to this decomposition the core-polarization propagator can be written as

$$\Pi = (G_c^0 + R_c + K_c) * (G_v^0 + R_v + K_v) ,$$

where the product * means either a simple product (unlinked diagrams) or a connection via the core potential (linked diagrams). The indices c and v refer to core and valence, respectively. Π can now be written as the sum of a zeroth-order term (HF), a relaxation term and a correlation term according to

$$\Pi = G_c^0 \cdot G_v^0 + (G_c^0 * R_v + R_c \cdot G_v^0 + R_c * R_v) + (G_c^0 * K_v + K_c \cdot G_v^0 + R_c * K_v + K_c * R_v + K_c * K_v) ,$$

where the dot denotes a simple product (unlinked diagrams). The diagrams of R_v leading to unlinked diagrams of Π are at least of second order, whereas for a linked diagram of Π they can be of first order. Analogously, K_v must be at least of second or third order to yield unlinked or linked diagrams of Π, respectively. The diagrams of R_c (or K_c) yield, on the other hand, unlinked as well as linked diagrams of Π if they are of at least second (or third) order. This order analysis is illustrated in Table I. In the last column we have listed some examples of second-order diagrams. Higher-order diagrams can now easily be constructed from Table I as, e.g., the third-order diagrams of Π originating from $(R_c * R_v)_L$ which is drawn in Fig. 8. It is seen that several new classes of diagrams have to be considered if the analytical decomposition of the core-valence excitation energy is extended beyond second-order.

TABLE I. Decomposition of the core polarization propagator into the various relaxation and correlation parts.

Contribution to Π	Reorganization and correlation	Linked and unlinked	Order ($\geqslant$)	Examples (second order) (see Fig. 7)
$G_c^0 \cdot G_v^0$	HF	u	$=0$	
$G_c^0 * R_v$	R	u	2	(b)
		l	1	(a), (e), (f), (g), (h)
$R_c \cdot G^0$	R	u	2	(c), (d)
$R_c * R_V$	R	u	4	
		l	3	
$G_c^0 * K_v$	C	u	2	(i, j)
		l	3	
$K_c \cdot G_v^0$	C	u	3	
$R_c * K_v$	C	u	4	
		l	5	
$K_c * R_v$	C	u	5	
		l	4	
$K_c * K_v$	C	u	5	
		l	6	

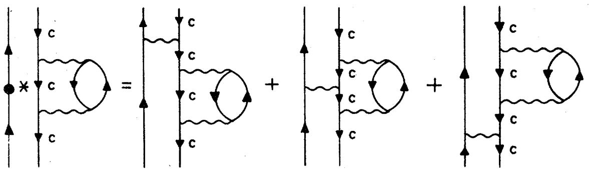

FIG. 8. Example of diagrams of Π which belong to $(R_c{*}R_v)_L$.

IV. AN ILLUSTRATIVE EXAMPLE

In order to illustrate the factorization theorem we present an exact calculation of the core polarization propagator for a simple model. Consider a system consisting of a core orbital ϕ_c, an occupied valence orbital ϕ_o, and an unoccupied orbital ϕ_u. Our Hamiltonian reads[24]

$$H_{cv}=\sum_{\alpha}(\epsilon_c\hat{n}_{c\alpha}+\epsilon_o\hat{n}_{o\alpha}+\epsilon_u\hat{n}_{u\alpha})$$
$$-V\sum_{\alpha,\beta}(1-\hat{n}_{c\alpha})(a^{\dagger}_{o\beta}a_{u\beta}+a^{\dagger}_{u\beta}a_{o\beta}), \tag{55}$$

where α, β denote the spin indices. The second term describes the interaction between a particle and a hole due to the core hole potential. Obviously this Hamiltonian contains no ground-state correlation.

Let us now consider the case of core-valence excitations. The excited state is described by the two configurations

$$|1\rangle=2^{-1/2}(a^{\dagger}_{u\alpha}a_{c\alpha}+a^{\dagger}_{u\beta}a_{c\beta})\,|\Phi_0\rangle$$

and (56)

$$|2\rangle=2^{-1/2}(a^{\dagger}_{u\alpha}a_{c\alpha}a^{\dagger}_{u\beta}a_{o\beta}+a^{\dagger}_{u\beta}a_{c\beta}a^{\dagger}_{u\alpha}a_{o\alpha})\,|\Phi_0\rangle ,$$

where $|\Phi_0\rangle$ denotes the noncorrelated ground state. Since the configurational space is very limited, the configuration-interaction approach is rather useful and the solution of our problem is obtained by diagonalizing the following matrix:

$$A=\begin{bmatrix}-\epsilon_c+\epsilon_u & -V\\ -V & -\epsilon_c+\epsilon_u+\Delta\end{bmatrix}. \tag{57}$$

Δ denotes the zeroth-order particle-hole excitation energy $\epsilon_u-\epsilon_o$. The ground-state energy $E_0=2\epsilon_c+2\epsilon_o$ has been subtracted from the diagonal elements. The corresponding transition probabilities are identical to the squares of the first element of the eigenvectors. Thus, the core-polarization propagator $\Pi_{ucuc}(\omega)$ reads

$$\Pi_{ucuc}(\omega)=\frac{(a+\Delta)/2a}{\omega+\epsilon_c-\epsilon_u-\frac{1}{2}(a-\Delta)+i\eta}+\frac{(a-\Delta)/2a}{\omega+\epsilon_c-\epsilon_u-\frac{1}{2}(a+\Delta)+i\eta}, \tag{58}$$

where $a=(\Delta^2+4V^2)^{1/2}$.

The diagrammatic approach to this problem is not so easy to carry out. This is not at all surprising. The many-body techniques have been derived for the approximate solution of "many-state" problems involving large numbers of electrons for which the configuration-interaction method is not attractive or even inapplicable. The diagrammatic solution of a simple "two-state" system is extremely complicated in comparison to the quadratic equation arising in the configuration-interaction approach. The diagrams of Π up to the 4th order in V are shown for our model system in Fig. 9. We may proceed by introducing the core-interaction points into the diagrams. In this way most of the diagrams become unlinked such that we can draw the expansion as a product of two sums of linked diagrams. This factorization is demonstrated in Fig. 10 and leads to the factorization theorem (29):

$$(-i)\Pi_{ucuc}(t)=i\rho_{uu}(t)iG_{cc}(-t), \tag{59}$$

where the limit τ to t has already been taken and

$$\rho_{uu}(t)=\lim_{\tau\to t}\rho_{uu}(t;\tau). \tag{60}$$

The function $\rho_{uu}(t;\tau)$ is an element of the matrix $\rho(t;\tau)$ which satisfies the Dyson equation (46)

$$\rho(t;\tau)=G^0(t)+\int dt_1\int dt_2G^0(t-t_1)\Sigma(t_1,t_2;\tau)\rho(t_2;\tau), \tag{61}$$

where the quantities represent 2×2 matrices

$$\rho(t;\tau)=\begin{bmatrix}\rho_{oo}(t;\tau)\rho_{ou}(t;\tau)\\ \rho_{uo}(t;\tau)\rho_{uu}(t;\tau)\end{bmatrix},$$

$$G^0(t)=\begin{bmatrix}G^0_o(t) & 0\\ 0 & G^0_u(t)\end{bmatrix}, \tag{62}$$

and

$$\Sigma(t_1,t_2)=\begin{bmatrix}0 & V\\ V & 0\end{bmatrix}\delta(t_1-t_2)\Theta(\tau-t_1)\Theta(t_1).$$

This yields a coupled set of integral equations. Since we are interested in the function $\rho_{uu}(t;\tau)$ we have to solve the following equations:

$$\rho_{uu}(t;\tau)=G^0_u(t)+\int dt_1G^0_u(t-t_1)V\Theta(\tau-t_1)\Theta(t_1)\rho_{ou}(t;\tau), \tag{63a}$$

$$\rho_{ou}(t;\tau)=\int dt_1G^0_o(t-t_1)V\Theta(\tau-t_1)\Theta(t_1)\rho_{uu}(t_1;\tau). \tag{63b}$$

Equations (63a) and (63b) can be combined to the integral equation

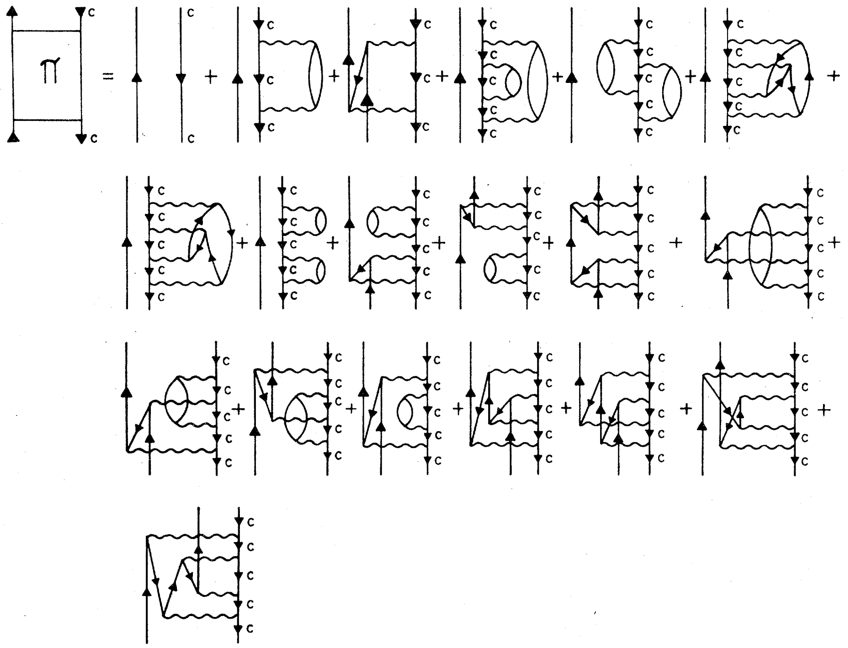

FIG. 9. Diagrammatic expansion of $\Pi_{ucuc}(t,-\tau)$ up to fourth order for the model.

$$\rho_{uu}(t;\tau)=G_u^0(t)+V^2\int_0^t dt_1\int_{t_1}^{\tau} dt_2 G_u^0(t-t_1)\times G_o^0(t_1-t_2)\rho_{uu}(t_2;\tau)\,, \tag{64}$$

where we have restricted ourselves to $\tau \geqslant t$. The solution of Eq. (64) has been given in Ref. 24 and is obtained by converting it into a differential equation. The final result reads

$$\rho_{uu}(t;\tau)=e^{-i(\epsilon_0+\epsilon_u)t/2}[K_1(\tau)e^{iat/2}+K_2(\tau)e^{-iat/2}], \tag{65}$$

where the coefficients $K_i(\tau)$ are determined by inserting Eq. (65) into the integral equation (64). When $\tau \to t$, Eq. (60) reads

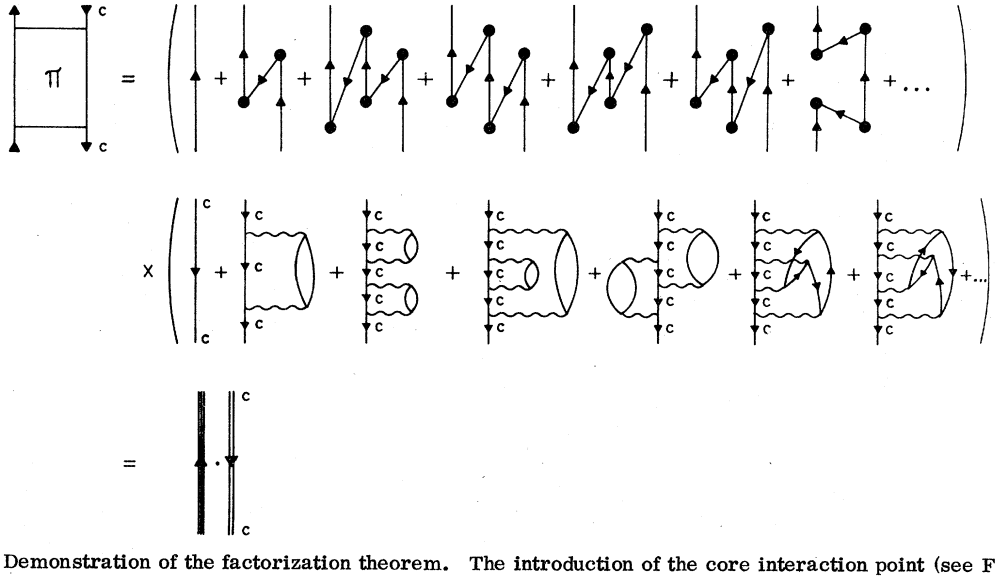

FIG. 10. Demonstration of the factorization theorem. The introduction of the core interaction point (see Fig. 1) enables us to write the diagrams of Π as products of two one-particle Green's functions. In the core Green's function we have used the interaction wiggle to demonstrate the difference to the other Green's function.

$$i\rho_{uu}(t) = 2ae^{-i(\epsilon_o+\epsilon_u)t/2}\,[(a+\Delta)e^{iat/2}+(a-\Delta)e^{-iat/2}]^{-1}\,. \tag{66}$$

It is obvious that the rather simple dependence of $\rho_{uu}(t;\tau)$ on the variable t has been destroyed by the coefficients $K_i(t)$ which originate from the time-dependent core potential. $\rho_{uu}(t)$ has indeed a very complicated analytical structure.

The core Green's function $G_{cc}(t)$ is obtained by using the linked cluster theorem[24] (35)

$$G_{cc}(t) = i\Theta(-t)e^{-i\epsilon_c t}e^{C(t)}\,. \tag{67}$$

The explicit calculation has been performed in Ref. 24. The final expression for the core Green's function reads

$$iG_{cc}(-t) = -\Theta(t)\left(\frac{(a+\Delta)^2}{4a^2}\,e^{i(\epsilon_c-\Delta+a)t}+\frac{(a-\Delta)^2}{4a^2}\,e^{i(\epsilon_c-\Delta-a)t}+\frac{2V^2}{a^2}\,e^{i(\epsilon_c-\Delta)t}\right). \tag{68}$$

A trivial algebraic manipulation shows that the core Green's function can be factorized according to

$$iG_{cc}(-t) = -\Theta(t)\left(\frac{a+\Delta}{4a^2}\,e^{i(\epsilon_c-\Delta+a/2)t}+\frac{a-\Delta}{4a^2}\,e^{i(\epsilon_c-\Delta-a/2)t}\right)[(a+\Delta)e^{iat/2}+(a-\Delta)e^{-iat/2}]\,, \tag{69}$$

where the second factor in brackets exactly cancels the denominator of $\rho_{uu}(t)$. The core polarization propagator is now given by

$$\Pi_{ucuc}(t) = -\,i\Theta(t)\left(\frac{a+\Delta}{2a}\,e^{i[\epsilon_c-\epsilon_u-(a-\Delta)/2]t}+\frac{a-\Delta}{2a}\,e^{i[\epsilon_c-\epsilon_u-(a+\Delta)/2]t}\right). \tag{70}$$

A Fourier transformation recovers Eq. (58).

It is interesting to convert Eq. (59) to ω space and insert the transformed Green's functions. While the Fourier transformation of the core Green's function is trivial, the valence Green's function $\rho_{uu}(t)$ has a rather complicated spectral representation. The denominator of Eq. (66) can be converted to

$$\frac{1}{a+\Delta}\,e^{-iat/2}\left(1+\frac{a-\Delta}{a+\Delta}\,e^{-iat}\right)^{-1}.$$

Next we expand the term in brackets and obtain for $\rho_{uu}(t)$

$$i\rho_{uu}(t) = \Theta(t)\frac{2a}{a+\Delta}\times\sum_{n=0}^{\infty}(-1)^n\left(\frac{a-\Delta}{a+\Delta}\right)^n e^{-i[(\epsilon_o+\epsilon_u+a)/2+an]t}\,. \tag{71}$$

The Fourier transformation yields

$$\rho_{uu}(\omega) = \frac{2a}{a+\Delta}\sum_{n=0}^{\infty}\frac{(-1)^n\left(\dfrac{a-\Delta}{a+\Delta}\right)^n}{\omega-\frac{1}{2}(\epsilon_o+\epsilon_u+a)-an+i\eta}\,. \tag{72}$$

Thus, we have found that already in this simple model the valence Green's function $\rho_{uu}(t)$ has infinitely many poles with *alternating* pole strengths converging to zero with increasing n. $\rho_{uu}(\omega)$ satisifies the following relation

$$\rho_{uu}(\omega)\to 1/\omega \tag{73}$$

for $\omega\to\infty$. Obviously nearly all poles must cancel when $\rho_{uu}(\omega)$ is convoluted with $G_{cc}(\omega)$ to obtain the polarization function $\Pi_{ucuc}(\omega)$. This is quaranteed by the sign change. It is interesting to note that the cancellation of poles via the product in t space occurs in ω space via the compensation of infinite sums.

Our model spectral function has been found to have the structure

$$\Pi(t)\simeq e^{C(-t)}(1+\alpha e^{-iat})^{-1} = e^{C(-t)}\sum_n(-\alpha)^n e^{-iant}\,, \tag{74}$$

which can formally be compared to the theory of Chang and Langreth[4] on deep-hole excitations in solids. Their spectral function possesses a similar structure given by

$$N(t)\simeq\exp(\beta e^{-iat})(1-\alpha e^{-iat})^{-1}\,. \tag{75}$$

Physically, the processes described by Chang and Langreth can be described as follows. A high-energy photon impinges on a solid exciting a core electron which then escapes. We consider first the propagation of the core hole. The modification of the spectral density of the deep hole left behind when the photoelectron is excited is called an intrinsic effect and is represented by the exponential in Eq. (75). The second effect concerns the propagation of the excited photoelectron. Its energy loss via inelastic scattering processes during the propagation is called extrinsic effect and is represented by the second quantity in parentheses. This leads to the formation of satellites. The strength of each successive satellite associated with the extrinsic effect falls off geometrically and is equal to α^n, where α is the probability that in a given interaction the electron emits a plasmon. The overall propagation is described by

$N(t)$ and represents an interference between the intrinsic and extrinsic effects.

In our theory we consider the excitations of core electrons to valence orbitals in atoms and molecules. The propagation of the core hole is discussed first. The modification of the spectral density of the deep hole upon excitations is described by the core Green's function which is mainly given by $e^{C(-t)}$. We may call this an intrinsic effect. If the boson approximation is applicable it has been shown[24] that $C(-t)$ is indeed given by an exponential function in complete analogy to the theory of Chang and Langreth. The other process taking place in our system concerns the propagation of the valence electron. This electron interacts with the other valence electrons and with the core hole. This is described by the valence Green's function $\rho(t)$ with the time-dependent core potential which is mainly given by the quantity in brackets in Eq. (74). Except the different sign of α this quantity is formally identical to the corresponding term in Eq. (75) and we may call it an extrinsic effect. It leads again to the formation of satellites. The strength of each successive satellite falls off geometrically but is identical to $(-\alpha)^n$. Hence we have alternating probabilities to excite satellites accounting for compensation (absorption) effects which are not present in the case discussed by Chang and Langreth. The final result is again an interference between intrinsic and extrinsic effects but because of the alternating sign of α a cancellation of nearly all poles occurs.

V. CONCLUSIONS

Theoretically the core-valence excitation spectrum can be determined using the full electronic Hamiltonian and solving the Bethe-Salpeter equation for the particle-hole component of the two-particle Green's function. The solution of this multiple integral equation is, however, a complicated problem. It is shown that the physical concept simplifies considerably when a Hamiltonian is employed which has been derived[24] by making explicit use of the deep core hole properties. In this case a factorization theorem can be proven for the particle-hole propagator decomposing it into a core Green's function and a valence Green's function. Hence we have reduced the problem of evaluating a two-particle Green's function to the problem of evaluating two one-particle Green's functions. The core ionization and the valence attachment can be treated independently, but at the cost of introducing a time-dependent core potential into the Hamiltonian of the valence Green's function. The latter function satisfies a Dyson equation whose self-energy part contains in addition to the usual interaction potential between the valence electrons the time-dependent core potential. Although the introduction of this time-dependent core potential into the valence Green's function leads to a complicated mathematical theory, the interpretation of this function in terms of diagrams remains both simple and vivid.

The self-energy can be decomposed into a part containing only core interactions and a part containing the rest. According to this decomposition the original Dyson equation is equivalent to a pair of Dyson equations. The first of these equations determines a valence Green's function containing only core interactions and hence possesses already the correct analytical time structure exhibited by the exact valence Green's function. It contains the main part of the reorganization and serves as the unperturbed Green's function in the second Dyson equation. It should be noted that the presence of the external core potential makes it impossible to convert the Dyson equations to simple algebraic equations in ω space.

The core-valence excitation energy has been decomposed into relaxation and correlation terms up to second order. These different contributions can be interpreted in terms of diagrams relating them to simple physical processes as, among others, relaxation of the orbitals in the presence of the additional core hole or valence particle, respectively. It is interesting to remark that in second order the entire correlation energy originates from the additional particle in the valence orbital. The existence of the core hole leads to a modification of the valence correlation energy in third order. A general order analysis of the core-valence excitation energy in terms of diagrams has been performed using the factorization theorem. In this way one can extend the decomposition of the energy into relaxation and correlation contributions beyond second order.

Starting from an exactly soluable model Hamiltonian considering only certain reorganization effects due to the core potential, the core-polarization propagator has been evaluated explicitly via the factorization theorem where the core Green's function and the valence Green's function have been calculated separately. It is shown that in time-space the valence Green's function is equal to a quotient of exponential functions. A spectral representation has been derived and it is clearly demonstrated that the simple ω dependence of the usual Green's function is completely destroyed. Even in the case of our simple model this function has infinitely many poles with *alternating* pole strengths. Nearly all of these poles cancel when this function is convoluted with the core Green's function. Thus, our model represents a simple physical picture of the processes involved in the core-valence excitation processes. It has also been shown that our theory of core-valence excitations of atoms and molecules is closely related to the theory of x-ray emission spectra of solids.

From the preceeding discussion of the core-valence excitation it is clear that although the physical concept has been simplified by the factorization theorem an explicit calculation is by no means a trivial problem. Anyway, our analysis yields an insight into the nature of the physical processes arising in connection with excitations from deep core orbitals. The excitation is split up into a core ionization and a valence attachment. Since these processes are not completely independent, this separation leads to the introduction of the time-dependent core potential into the Hamiltonian of the valence Green's function. Although the valence Green's function is difficult to determine for any realistic physical system, our analysis is a first step towards a solution and the next task will be the derivation of an appropriate approximation for this function. As has been shown[24] the core Green's function is also connected with the valance Green's function $\rho(t;\tau)$. The linked cluster theorem states that the core Green's function is given mainly by the exponential function of a quantity $C(t)$. This function $C(t)$ is related to the valence Green's function $\rho(t;\tau)$ and in the case of our model Hamiltonian (55) it is simply given by an integral over a product of two valence Green's functions. Therefore, the knowledge of the valence Green's function $\rho(t;\tau)$ is of importance for any further consideration of the core problem.

APPENDIX A

In this section an analytical proof of the factorization theorem Eq. (29) discussed in Sec. IIIC is presented. We consider the Hamiltonian (24) without the spin-flip term

$$H_{\mathrm{cv}}=H_{\mathrm{c}}+H_{\mathrm{v}}+W_{\mathrm{cv}}\,. \tag{A1}$$

$\tilde{H}_0=\sum_m \epsilon_m \hat{n}_m$ is our unperturbed Hamiltonian. The function $\Pi_{icjc}(t,-\tau)$ of Eq. (6) can be written as[10,12]

$$\Pi_{icjc}(t,-\tau)=\lim_{T_1\to-\infty,\,T_2\to+\infty} Q_\pi(T_2,T_1,t,-\tau)\,, \tag{A2}$$

where

$$Q_\pi(T_2,T_1,t,-\tau)$$

$$=-i\frac{\langle\Phi_0^N|T[\tilde{U}(T_2,T_1)\bar{a}_c^\dagger(\tau)\bar{a}_i(t)\bar{a}_j^\dagger\bar{a}_c]\,|\Phi_0^N\rangle}{\langle\Phi_0^N|\tilde{U}(T_2,T_1)|\Phi_0^N\rangle}\,. \tag{A3}$$

$|\Phi_0^N\rangle$ is the ground state of $\tilde{H}_0$, $\bar{O}$ is an operator O in the interaction picture

$$\bar{O}(t)=e^{i\tilde{H}_0 t}Oe^{-i\tilde{H}_0 t}\,, \tag{A4}$$

and $\tilde{U}(T_1,T_2)$ is the time-development operator

$$\tilde{U}(T_2,T_1)=e^{i\tilde{H}_0T_2}e^{-iH_{\mathrm{cv}}(T_2-T_1)}e^{-i\tilde{H}_0T_1}\,. \tag{A5}$$

After some straightforward algebraic manipulations we can eliminate all core operators from (A3) and we obtain for the time ordering $T_2\geqslant\tau\geqslant t\geqslant 0\geqslant T_1$ the following expression for Q_π:

$$Q_\pi(T_2,T_1,t,-\tau)=-ie^{i\epsilon_c\tau}\frac{\langle\Phi_0^{N_v}|e^{-iH_v(T_2-\tau)}e^{-i(H_v+V_1)(\tau-t)}a_ie^{-i(H_v+V_1)t}a_j^\dagger e^{iH_vT_1}|\Phi_0^{N_v}\rangle}{\langle\Phi_0^{N_v}|e^{-iH_v(T_2-T_1)}|\Phi_0^{N_v}\rangle}\,, \tag{A6a}$$

and for the other time ordering $T_2\geqslant t\geqslant\tau\geqslant 0\geqslant T_1$,

$$Q_\pi(T_2,T_1,t,-\tau)=-ie^{i\epsilon_c\tau}\frac{\langle\Phi_0^{N_v}|e^{-iH_v(T_2-t)}a_ie^{-iH_v(t-\tau)}e^{-i(H_v+V_1)\tau}a_j^\dagger e^{iH_vT_1}|\Phi_0^{N_v}\rangle}{\langle\Phi_0^{N_v}|e^{-iH_v(T_2-T_1)}|\Phi_0^{N_v}\rangle}\,. \tag{A6b}$$

$|\Phi_0^{N_v}\rangle$ denotes the ground state of the unperturbed valence electron operator $H_0=\sum_i\epsilon_i\hat{n}_i$ $(i\neq c)$, $H_v=H_0+V_v$, and V_1 is given by

$$V_1=-\sum_{ij}V_{ic[jc]}(a_i^\dagger a_j-n_i\delta_{ij})\,. \tag{A7}$$

Next we introduce two time-development operators for the valence electrons, one $(\tilde{U}_0)$ for the ground state and one $(\tilde{U}_1)$ for the core hole states,

$$\tilde{U}_0(T_2,T_1)=e^{iH_0T_2}e^{-iH_v(T_2-T_1)}e^{-iH_0T_1}\,, \tag{A8a}$$

$$\tilde{U}_1(T_2,T_1)=e^{iH_0T_2}e^{-i(H_v+V_1)(T_2-T_1)}e^{-iH_0T_1}\,. \tag{A8b}$$

Using these operators we can rewrite (A6a) and (A6b) as

$$Q_\pi(T_2,T_1,t,-\tau)=-ie^{i\epsilon_c\tau}\frac{\langle\Phi_0^{N_v}|\tilde{U}_0(T_2,\tau)\tilde{U}_1(\tau,t)\bar{a}_i(t)\tilde{U}_1(t,0)\bar{a}_j^\dagger\tilde{U}_0(0,T_1)|\Phi_0^{N_v}\rangle}{\langle\Phi_0^{N_v}|\tilde{U}_0(T_2,T_1)|\Phi_0^{N_v}\rangle}\,, \tag{A9a}$$

$$Q_\pi(T_2,T_1,t,-\tau)=-ie^{i\epsilon_c\tau}\,\frac{\langle\Phi_0^{N_v}|\tilde{U}_0(T_2,t)\bar{a}_i(t)\tilde{U}_0(t,\tau)\tilde{U}_1(\tau,0)\bar{a}_j^\dagger\tilde{U}_0(0,T_1)|\Phi_0^{N_v}\rangle}{\langle\Phi_0^{N_v}|\tilde{U}_0(T_2,T_1)|\Phi_0^{N_v}\rangle}, \tag{A9b}$$

where $\bar{O}$ is again an operator in the interaction picture given now by

$$\bar{O}(t)=e^{iH_0t}Oe^{-iH_0t}. \tag{A10}$$

We proceed by defining the operator $\tilde{U}_\tau(T'',T')$ via the expansion

$$\tilde{U}_\tau(T'',T')=\sum_{n=0}^{\infty}\frac{(-i)^n}{n!}\int_{T'}^{T''}dt_1\cdots\times\int_{T'}^{T''}dt_n T[\bar{V}(t_1)\cdots\bar{V}(t_n)], \tag{A11}$$

where

$$\bar{V}(t_i)=\bar{V}_v(t_i)+\bar{V}_1(t_i)\Theta(\tau-t_i)\Theta(t_i). \tag{A12}$$

It is obvious that the following relations hold:

$$\tilde{U}_0(T_2,\tau)=\tilde{U}_\tau(T_2,\tau),$$

$$\tilde{U}_1(\tau,0)=\tilde{U}_\tau(\tau,0),$$

$$\tilde{U}_0(0,T_1)=\tilde{U}_\tau(0,T_1).$$

The operator $\tilde{U}_\tau(T'',T')$ is a time-development operator for the time-dependent perturbation

$$V(t)=V_v+V_1\Theta(\tau-t)\Theta(t).$$

Using this operator we can combine Eqs. (A9a) and (A9b),

$$\begin{aligned}Q_\pi=(T_2,T_1,t,-\tau)&=-ie^{i\epsilon_c\tau}\frac{\langle\Phi_0^{N_v}|\tilde{U}_\tau(T_2,t)\bar{a}_i(t)\tilde{U}_\tau(t,0)\bar{a}_j^\dagger\tilde{U}_\tau(0,T_1)|\Phi_0^{N_v}\rangle}{\langle\Phi_0^{N_v}|\tilde{U}_0(T_2,T_1)|\Phi_0^{N_v}\rangle}\\&=-ie^{i\epsilon_c\tau}\frac{\langle\Phi_0^{N_v}|T[\tilde{U}_\tau(T_2,T_1)\bar{a}_i(t)\bar{a}_j^\dagger]|\Phi_0^{N_v}\rangle}{\langle\Phi_0^{N_v}|\tilde{U}_0(T_2,T_1)|\Phi_0^{N_v}\rangle}.\end{aligned} \tag{A13}$$

Correspondingly the core Green's function reads[10]

$$G_{cc}(-\tau)=\lim_{T_1\to-\infty,T_2\to+\infty}Q_c(T_2,T_1,-\tau), \tag{A14}$$

and Q_c can be written as[24]

$$Q_c(T_2,T_1,-\tau)=ie^{i\epsilon_c\tau}\frac{\langle\Phi_0^{N_v}|\tilde{U}_\tau(T_2,T_1)|\Phi_0^{N_v}\rangle}{\langle\Phi_0^{N_v}|\tilde{U}_0(T_2,T_1)|\Phi_0^{N_v}\rangle}. \tag{A15}$$

Thus, defining a new quantity Q_v by

$$Q_v(T_2,T_1,t,\tau)=i\frac{Q_\pi(T_2,T_1,t,-\tau)}{Q_c(T_2,T_1,-\tau)}, \tag{A16}$$

we finally obtain

$$Q_v(T_2,T_1,t,\tau)=-i\,\frac{\langle\Phi_0^{N_v}|T[\tilde{U}_\tau(T_2,T_1)\bar{a}_i(t)\bar{a}_j^\dagger]|\Phi_0^{N_v}\rangle}{\langle\Phi_0^{N_v}|\tilde{U}_\tau(T_2,T_1)|\Phi_0^{N_v}\rangle}, \tag{A17}$$

which introduces a new Green's function

$$i\rho_{ij}(t;\tau)=\lim_{T_1\to-\infty,T_2\to+\infty}\frac{\langle\Phi_0^{N_v}|T[\tilde{U}_\tau(T_2,T_1)\bar{a}_i(t)\bar{a}_j^\dagger]|\Phi_0^{N_v}\rangle}{\langle\Phi_0^{N_v}|\tilde{U}_\tau(T_2,T_1)|\Phi_0^{N_v}\rangle}, \tag{A18}$$

which will be shown to be a valence Green's function with a time-dependent core potential. The function $\Pi_{icjc}(t,-\tau)$ satisfies a factorization theorem

$$(-i)\Pi_{icjc}(t,-\tau)=i\rho_{ij}(t;\tau)iG_{cc}(-\tau). \tag{A19}$$

The core polarization propagator $\Pi_{icjc}(t)$ is obtained from Eq. (A19) by taking the limit $\tau\to t$

$$\begin{aligned}\Pi_{icjc}(t)&=\lim_{\tau\to t}\Pi_{icjc}(t,-\tau)\\&=-i\rho_{ij}(t)G_{cc}(-t).\end{aligned} \tag{A20}$$

This factorization implies that the core-valence excitation process can be decomposed into two different simultaneously occurring processes, namely a core-ionization process and a valence attachment in the field of the core potential. The physical meaning of this decomposition is discussed in detail in Sec. IIIC. Finally, it should be noted that a reversal of the time variables ($t\to-t$, $-\tau\to\tau$) leaves Π invariant and thus leads to the same results.

APPENDIX B

In this section we derive the Heisenberg representation for $\rho_{ij}(t;\tau)$. We start from the definition of $\rho_{ij}(t;\tau)$ in the interaction picture derived in Appendix A (A18)

$$i\rho_{ij}(t;\tau)=\frac{\langle\Phi_0^{N_v}|T[\tilde{U}_\tau(+\infty,-\infty)\bar{a}_i(t)\bar{a}_j^\dagger]|\Phi_0^{N_v}\rangle}{\langle\Phi_0^{N_v}|\tilde{U}_\tau(+\infty,-\infty)|\Phi_0^{N_v}\rangle}, \tag{B1}$$

where all quantities have been defined in Appendix A (with $\tau \geqslant 0$). We consider the time ordering $t \geqslant 0$ and write

$$i\rho_{ij}(t;\tau) = \frac{\langle \Phi_0^{N_v} | \tilde{U}_\tau(+\infty,0)\tilde{U}_\tau(0,t)\overline{a}_i(t)\tilde{U}_\tau(t,0)\overline{a}_j^\dagger \tilde{U}_\tau(0,-\infty) | \Phi_0^{N_v}\rangle}{\langle \Phi_0^{N_v} | \tilde{U}_\tau(+\infty,0)\tilde{U}_\tau(0,-\infty) | \Phi_0^{N_v}\rangle} . \tag{B2}$$

Defining the states

$$\begin{aligned} \langle \Psi_0^{N_v}(\tau) | &= \langle \Phi_0^{N_v} | \tilde{U}_\tau(+\infty, 0) , \\ | \Psi_0^{N_v}\rangle &= \tilde{U}_\tau(0,-\infty) | \Phi_0^{N_v}\rangle , \end{aligned} \tag{B3}$$

we can write

$$i\rho_{ij}(t;\tau) = \frac{\langle \Psi_0^{N_v}(\tau) | \tilde{U}_\tau(0,t)\overline{a}_i(t)\tilde{U}_\tau(t,0)\overline{a}_j^\dagger | \Psi_0^{N_v}\rangle}{\langle \Psi_0^{N_v}(\tau) | \Psi_0^{N_v}\rangle} . \tag{B4}$$

It should be noted that if the time-dependent potential is neglected, the above defined states $|\Psi_0^{N_v}(\tau)\rangle$ and $|\Psi_0^{N_v}\rangle$ become identical. In the Heisenberg representation the operator a_i is given by

$$\begin{aligned} a_i(t) &\equiv \tilde{U}_\tau(0,t)\overline{a}_i(t)\tilde{U}_\tau(t,0) \\ &= \tilde{U}_\tau^{-1}(t,0)e^{iH_0t}a_i e^{-iH_0t}\tilde{U}_\tau(t,0) \\ &\equiv U_\tau^{-1}(t)a_i U_\tau(t) , \end{aligned} \tag{B5}$$

where $U_\tau(t) \equiv e^{-iH_0t}\tilde{U}_\tau(t,0)$. This leads to the following expression in the Schrödinger picture:

$$i\rho_{ij}(t;\tau) = \frac{\langle \Psi_0^{N_v}(\tau) | \tilde{U}_\tau^{-1}(t)a_i\tilde{U}_\tau(t)a_j^\dagger | \Psi_0^{N_v}\rangle}{\langle \Psi_0^{N_v}(\tau) | \Psi_0^{N_v}\rangle} , \tag{B6}$$

and in the Heisenberg picture,

$$i\rho_{ij}(t;\tau) = \frac{\langle \Psi_0^{N_v}(\tau) | a_i(t)a_j^\dagger | \Psi_0^{N_v}\rangle}{\langle \Psi_0^{N_v}(\tau) | \Psi_0^{N_v}\rangle} . \tag{B7}$$

The analogous expression can be derived for the other time ordering $t \leqslant 0$ and finally we arrive at

$$i\rho_{ij}(t;\tau) = \frac{\langle \Psi_0^{N_v}(\tau) | T[a_i(t)a_j^\dagger] | \Psi_0^{N_v}\rangle}{\langle \Psi_0^{N_v}(\tau) | \Psi_0^{N_v}\rangle} . \tag{B8}$$

APPENDIX C

In this section we derive analytical expressions for $\rho_{ij}(t;\tau)$ and $\rho_{ij}(t)$ which exhibit explicitly their time dependence. We start from Eq. (B1) of Appendix B and consider here only the time ordering $t, \tau \geqslant 0$. Let us first consider the case $t \leqslant \tau$ and define $|\Psi_0^{N_v}\rangle = \tilde{U}_0(0, \pm\infty) | \Phi_0^{N_v}\rangle$. Then we obtain

$$i\rho_{ij}(t;\tau) = \frac{\langle \Psi_0^{N_v} | \tilde{U}_0(0,\tau)\tilde{U}_1(\tau,t)\overline{a}_i(t)\tilde{U}_1(t,0)\overline{a}_j^\dagger | \Psi_0^{N_v}\rangle}{\langle \Psi_0^{N_v} | \tilde{U}_0(0,\tau)\tilde{U}_1(\tau,0) | \Psi_0^{N_v}\rangle} . \tag{C1}$$

We introduce the complete sets of eigenstates $\{|\Psi_n\rangle\}$ and $\{|\tilde{\Psi}_n\rangle\}$ which satisfy the following Schrödinger equations:

$$\begin{aligned} H_v |\Psi_n\rangle &= E_n |\Psi_n\rangle , \\ (H_v + V_1) |\tilde{\Psi}_n\rangle &= \tilde{E}_n |\tilde{\Psi}_n\rangle . \end{aligned}$$

Inserting the eigenstates $|\tilde{\Psi}_n\rangle$ into Eq. (C1) we obtain

$$i\rho_{ij}(t;\tau) = \sum_{n,m} C_{0n}(\tau) \langle \tilde{\Psi}_n^{N_v} | \tilde{U}_1(0,t)\overline{a}_i(t)\tilde{U}_1(t,0) | \tilde{\Psi}_m^{N_v+1}\rangle\langle \tilde{\Psi}_m^{N_v+1} | a_j^\dagger | \Psi_0^{N_v}\rangle , \tag{C2}$$

where $C_{0n}(\tau)$ is defined by

$$C_{0n}(\tau) = \frac{\langle \Psi_0^{N_v} | \tilde{U}_0(0,\tau)\tilde{U}_1(\tau,0) | \tilde{\Psi}_n^{N_v}\rangle}{\langle \Psi_0^{N_v} | \tilde{U}_0(0,\tau)\tilde{U}_1(\tau,0) | \Psi_0^{N_v}\rangle} . \tag{C3}$$

Using the definitions of the time-development operator $\tilde{U}_0(t,t_0)$ and $\tilde{U}_1(t,t_0)$, respectively, which are given in Appendix A, we obtain

$$i\rho_{ij}(t;\tau) = \sum_{n,m} C_{0n}(\tau) \langle \tilde{\Psi}_n^{N_v} | e^{i(H_v+V_1)t}a_i e^{-i(H_v+V_1)t} | \tilde{\Psi}_m^{N_v+1}\rangle\langle \tilde{\Psi}_m^{N_v+1} | a_j^\dagger | \Psi_0^{N_v}\rangle , \tag{C4}$$

$$i\rho_{ij}(t;\tau) = \sum_{n,m} e^{i(\tilde{E}_n^{N_v}-\tilde{E}_m^{N_v+1})t} C_{0n}(\tau) \langle \tilde{\Psi}_n^{N_v} | a_i | \tilde{\Psi}_m^{N_v+1}\rangle\langle \tilde{\Psi}_m^{N_v+1} | a_j^\dagger | \Psi_0^{N_v}\rangle . \tag{C5}$$

This equation shows explicitly the time dependence of $\rho_{ij}(t;\tau)$. The functions $C_{0n}(\tau)$ contain only the core hole "lifetime". Thus, the dependence on t and τ has been separated,

$$\rho(t;\tau) = \sum_n C_{0n}(\tau) f_n(t) . \tag{C6}$$

It is also important to exhibit the τ dependence of the coefficient $C_{0n}(\tau)$. Using Eq. (C3) we obtain

$$C_{0n}(\tau) = \frac{\langle \Psi_0^{N_v} | e^{iH_v\tau} e^{-i(H_v+V_1)\tau} | \tilde{\Psi}_n^{N_v}\rangle}{\langle \Psi_0^{N_v} | e^{iH_v\tau} e^{-i(H_v+V_1)\tau} | \Psi_0^{N_v}\rangle} . \tag{C7}$$

This leads to the result

$$C_{0n}(\tau)=\frac{e^{i(E_0^{N_v}-\tilde{E}_n^{N_v})\tau}\langle\Psi_0^{N_v}|\tilde{\Psi}_n^{N_v}\rangle}{\sum_k|\langle\Psi_0^{N_v}|\tilde{\Psi}_k^{N_v}\rangle|^2 e^{i(E_0^{N_v}-\tilde{E}_k^{N_v})\tau}}\,. \tag{C8}$$

Analogous equations are obtained for the case $\tau\leqslant t$,

$$i\rho_{ij}(t;\tau)=\sum_{n,m}e^{i(E_0^{N_v}-E_n^{N_v+1})t}\langle\Psi_0^{N_v}|a_i|\Psi_n^{N_v+1}\rangle C_{nm}(\tau)\times\langle\tilde{\Psi}_m^{N_v+1}|a_j^\dagger|\Psi_0^{N_v}\rangle\,, \tag{C9}$$

with

$$C_{nm}(\tau)=\frac{e^{i(E_n^{N_v+1}-\tilde{E}_m^{N_v+1})\tau}\langle\Psi_n^{N_v+1}|\tilde{\Psi}_m^{N_v+1}\rangle}{\sum_k|\langle\Psi_0^{N_v}|\tilde{\Psi}_k^{N_v}\rangle|^2 e^{i(E_0^{N_v}-\tilde{E}_k^{N_v})\tau}}\,. \tag{C10}$$

In the limit $\tau\rightarrow t$ both Eqs. (C5) and (C9) must lead to the same function $\rho_{ij}(t)$, i.e.,

$$\rho_{ij}(t)=\lim_{\tau\rightarrow t+\eta}\rho_{ij}(t;\tau)=\lim_{\tau\rightarrow t-\eta}\rho_{ij}(t;\tau) \tag{C11}$$

Indeed, both Eqs. (C5) and (C9) lead to

$$i\rho_{ij}(t)=\frac{\sum_m e^{i(E_0^{N_v}-\tilde{E}_m^{N_v+1})t}|\langle\tilde{\Psi}_m^{N_v+1}|a_j^\dagger|\Psi_0^{N_v}\rangle|^2}{\sum_k e^{i(E_0^{N_v}-\tilde{E}_k^{N_v})t}|\langle\tilde{\Psi}_k^{N_v+1}|\Psi_0^{N_v}\rangle|^2}\,. \tag{C12}$$

This expression can be interpreted as follows. Let us first consider the numerator. $\langle\tilde{\Psi}_m^{N_v+1}|a_j^\dagger|\Psi_0^{N_v}\rangle$ is the overlap matrix element between the valence ground state $|\Psi_0^{N_v}\rangle$ (without core potential), with an additional electron created in orbital j, and the excited state $|\tilde{\Psi}_m^{N_v+1}\rangle$ which is calculated in the presence of the core potential. This is identical to the probability amplitude for a core-valence transition. Correspondingly, the energy difference $E_0^{N_v}-\tilde{E}_m^{N_v+1}$ is just the core-valence excitation energy. The numerator of Eq. (C12) is, therefore, equal to the core-polarization propagator. Next we consider the denominator. $\langle\tilde{\Psi}_k^{N_v+1}|\Psi_0^{N_v}\rangle$ is the overlap matrix element between the valence ground state $|\Psi_0^{N_v}\rangle$ and the excited state $|\tilde{\Psi}_k^{N_v}\rangle$ which is calculated in the presence of the core potential. Hence, $|\tilde{\Psi}_n^{N_v}\rangle$ is identical to a state with a core hole. The energy difference $E_0^{N_v}-\tilde{E}_k^{N_v}$ is the corresponding ionization potential of the core electron. The denominator is, therefore, equal to the core Green's function.

Obviously, in the limit τ tending to t the simple time dependence of Eqs. (C5) and (C9) on t and τ has been destroyed. The complicated analytical structure of $\rho_{ij}(t)$ on t originates from the time-dependent coefficients $C_{0n}(t)$ and $C_{nm}(t)$, respectively. Although a formal spectral representation of $\rho_{ij}(t)$ can be derived we will not do it explicitly. We can separately transform t and τ to ω space by introducing the Fourier transform of $\rho_{ij}(t;\tau)$ by

$$\rho_{ij}(\omega';\omega'-\omega)=\int dt\,d\tau\,e^{i\omega' t}e^{i(\omega'-\omega)\tau}\rho_{ij}(t;\tau)\,. \tag{C13}$$

Then $\rho_{ij}(\omega)$ is given by

$$\rho_{ij}(\omega)=\int\frac{d\omega'}{2\pi}\rho_{ij}(\omega';\omega'-\omega)\,. \tag{C14}$$

Using Eq. (C6) we obtain the final result

$$\rho(\omega)=\sum_n\int\frac{d\omega'}{2\pi}C_{0n}(\omega'-\omega)f_n(\omega')\,, \tag{C15}$$

where $C_{0n}(\omega)$ and $f_n(\omega)$ are the Fourier transforms of $C_{0n}(\tau)$ and $f_n(t)$, respectively. For the other time ordering ($\tau\leqslant t$) one obtains an analogous result.

---

[1] E. E. Koch, in *Interaction of Radiation with Condensed Matter*, International Centre for Theoretical Physics, Winter College, 1976 (IAEA, Vienna, 1977), Vol. 2, pp. 225–274; R. Coisson, in *Imaging Processes and Coherence in Physics*, *Les Houches*, *1979*, edited by Ehlers, Hepp, Kippenhahn, Weidenmüller, Zittartz (Springer, Berlin, 1980); *Topics in Current Physics*, edited by C. Kunz (Springer, Berlin, 1979), Vol. 10, M. Nakamura, M. Sasanuma, S. Sato, M. Watanabe, H. Yamashita, Y. Iguchi, A. Ejiri, S. Nakai, S. Yamaguchi, I. Sagawa, Y. Nakai, and T. Oshio, Phys. Rev. 178, 80 (1969); W. Eberhardt, R. P. Haelbich, M. Iwan, E. E. Koch, and C. Kunz, Chem. Phys. Lett. 40, 180 (1976).

[2] G. C. King, M. Tronc, and F. H. Read, Chem. Phys. Lett. 52, 50 (1977); M. J. van der Wiel and Th. M. El Sherbini, Physica 59, 453 (1972); M. J. van der Wiel, Th. M. El Sherbini, and C. E. Brion, Chem. Phys. Lett. 7, 161 (1970); G. R. Wright, C. E. Brion, and M. J. van der Wiel, J. Electron Spectrosc. Relat. Phenom. 1, 475 (1972/73); G. R. Wright and C. E. Brion, *ibid.* 3, 191 (1974); 4, 25 (1974); 4, 327 (1974); 4, 335 (1974); 4, 347 (1974); M. Tronc, G. C. King, R. C. Bradford, and F. H. Read, J. Phys. B 9, L555 (1976); 12, 137 (1979); A. P. Hitchcock, M. Pocock, C. E. Brion, M. S. Banna, D. C. Frost, C. A. McDowell, and B. Wallbank, J. Electron Spectrosc. Relat. Phenom. 13, 345 (1978); A. P. Hitchcock and C. E. Brion, *ibid.* 13, 193 (1978); A. P. Hitchcock and C. E. Brion, Chem. Phys. Lett. 39, 588 (1976).

[3] P. Nozières and C. T. De Dominicis, Phys. Rev. 178, 1097 (1969).

[4] D. C. Langreth, Phys. Rev. B 1, 471 (1970); Phys. Rev. Lett. 26, 1229 (1971); J. J. Chang and D. C. Langreth, Phys. Rev. B 5, 3512 (1972); 8, 4638 (1973).

[5] *Modern Theoretical Chemistry, Electronic Structure: Ab initio Methods*, edited by H. F. Schaefer, III (Plenum, New York, 1976), Vol. II.

[6] W. Butscher, R. J. Buenker, and S. D. Peyerimhoff, Chem. Phys. Lett. 52, 449 (1977); W. H. E. Schwarz, W. Butscher, D. L. Ederer, T. B. Lucatorto, B. Ziegenbein, W. Mehlhorn, and H. Prömpeler, J. Phys. B

11, 591 (1978); A. Barth, S. D. Peyerimhoff, R. J. Buenker, and W. Butscher, Chem. Phys. 46, 149 (1980).

[7] R. J. Bartlett and I. Shavitt, Int. J. of Quantum. Chem. S11, 165 (1977).

[8] A. B. Migdal, *Theory of Finite Fermi Systems and Applications to Atomic Nuclei* (Interscience, New York, 1967).

[9] A. Abrikosov, L. Gorkov, and J. Dzyaloshinski, *Quantum Field Methods and Statistical Physics*, 2nd ed., edited by D. ter Haan (Pergamon, New York, 1965).

[10] A. L. Fetter and J. D. Walecka, *Quantum Theory of Many-Particle Systems* (McGraw-Hill, New York, 1971).

[11] D. J. Thouless, *The Quantum Mechanics of Many-Body Systems* (Academic, New York, 1961).

[12] R. D. Mattuck, *A Guide to Feynman Diagrams in the Many-Body Problem* (McGraw-Hill, New York, 1967).

[13] J. Linderberg and Y. Öhrn, *Propagators in Quantum Chemistry* (Academic, New York, 1973).

[14] L. S. Cederbaum and W. Domcke, Adv. Chem. Phys. 36, 205 (1977).

[15] G. Y. Csanak, H. S. Taylor, and R. Yaris, Adv. At. Mol. Phys. 7, 287 (1971).

[16] J. Paldus and J. Čížek, Adv. Quantum. Chem. 9, 105 (1973); J. Chem. Phys. 60, 149 (1974).

[17] J. Oddershede, Adv. Quantum. Chem. 11, 275 (1979); J. Oddershede and P. Jørgensen, J. Chem. Phys. 66, 1541 (1977).

[18] S. Ethofer and P. Schuck, Z. Phys. 228, 264 (1969); J. Winter, Nucl. Phys. A 194, 535 (1972).

[19] P. O. Löwdin, Adv. Chem. Phys. 14, 283 (1969).

[20] C. C. J. Roothaan, Rev. Mod. Phys. 23, 69 (1951); 32, 179 (1960).

[21] D. H. Kobe, Ann. Phys. (N. Y.) 19, 448 (1962).

[22] B. T. Pickup and O. Goscinski, Mol. Phys. 26, 1013 (1973).

[23] G. Born, H. A. Kurtz, and Y. Öhrn, J. Chem. Phys. 68, 74 (1978).

[24] L. S. Cederbaum, W. Domcke, and J. Schirmer, Phys. Rev. A 22, 206 (1980).